Plant Science 316 (2022) 111156

Contents lists available at ScienceDirect

Plant Science

journal homepage: www.elsevier.com/locate/plantsci

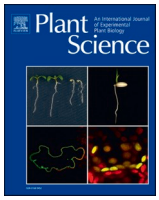

The jasmonate biosynthesis Gene *OsOPR7* can mitigate salinity induced mitochondrial oxidative stress

Kinfemichael Geressu Asfaw [a,*], Qiong Liu [a], Rose Eghbalian [a], Sabine Purper [a], Sahar Akaberi [a], Rohit Dhakarey [a], Stephan W. Münch [b,d], Ilona Wehl [b,d], Stefan Bräse [b,d], Elisabeth Eiche [f], Bettina Hause [g], Ivan Bogeski [c], Ute Schepers [b,e], Michael Riemann [a], Peter Nick [a,*]

[a] *Molecular Cell Biology, Botanical Institute, Karlsruhe Institute of Technology (KIT), Fritz-Haber-Weg 4, D-76131, Karlsruhe, Germany*
[b] *Institute of Organic Chemistry (IOC), Organic Chemistry I, Karlsruhe Institute of Technology (KIT), Fritz-Haber-Weg 6, D-76131, Karlsruhe, Germany*
[c] *Molecular Physiology, Institute of Cardiovascular Physiology, University Medical Center, Georg-August-University, 37073, Göttingen, Germany*
[d] *Institute of Biological and Chemical Systems-Functional Molecular Systems (IBCS-FMS), Karlsruhe Institute of Technology (KIT), Hermann-von-Helmholtz-Platz 1, D-76344, Eggenstein-Leopoldshafen, Germany*
[e] *Institute of Functional Interfaces (IFG), Karlsruhe Institute of Technology (KIT), Hermann-von-Helmholtz-Platz 1 D, 76344, Eggenstein-Leopoldshafen, Germany*
[f] *Institute of Applied Geochemistry (AGW), Geochemistry and Economic Geology Group, Karlsruhe Institute of Technology (KIT), Adenauerring 20b, D-76131, Karlsruhe, Germany*
[g] *Department of Cell and Metabolic Biology, Leibniz Institute of Plant Biochemistry, Weinberg 3, D-06120, Halle (Saale), Germany*

ARTICLE INFO

Keywords:
MnSOD
OPDA reductase
Cell penetrating peptoids
Plant mitochondria
Salt stress
Tobacco (*Nicotiana tabacum* L.) BY-2

ABSTRACT

Salinity poses a serious threat to global agriculture and human food security. A better understanding of plant adaptation to salt stress is, therefore, mandatory. In the non-photosynthetic cells of the root, salinity perturbs oxidative balance in mitochondria, leading to cell death. In parallel, plastids accumulate the jasmonate precursor *cis* (+)12-Oxo-Phyto-Dienoic Acid (OPDA) that is then translocated to peroxisomes and has been identified as promoting factor for salt-induced cell death as well. In the current study, we probed for a potential interaction between these three organelles that are primarily dealing with oxidative metabolism. We made use of two tools: (i) Rice OPDA Reductase 7 (OsOPR7), an enzyme localised in peroxisomes converting OPDA into the precursors of the stress hormone JA-Ile. (ii) A Trojan Peptoid, Plant PeptoQ, which can specifically target to mitochondria and scavenge excessive superoxide accumulating in response to salt stress. We show that overexpression of *OsOPR7* as GFP fusion in tobacco (*Nicotiana tabacum* L. cv. Bright Yellow 2, BY-2) cells, as well as a pretreatment with Plant PeptoQ can mitigate salt stress with respect to numerous aspects including proliferation, expansion, ionic balance, redox homeostasis, and mortality. This mitigation correlates with a more robust oxidative balance, evident from a higher activity of superoxide dismutase (SOD), lower levels of superoxide and lipid peroxidation damage, and a conspicuous and specific upregulation of mitochondrial SOD transcripts. Although both, Plant PeptoQ and ectopic OsOPR7, were acting in parallel and mostly additive, there are two specific differences: (i) OsOPR7 is strictly localised to the peroxisomes, while Plant PeptoQ found in mitochondria. (ii) Plant PeptoQ activates transcripts of NAC, a factor involved in retrograde signalling from mitochondria to the nucleus, while these transcripts are suppressed significantly in the cells overexpressing *OsOPR7*. The fact that overexpression of a peroxisomal enzyme shifting the jasmonate pathway from the cell-death signal OPDA towards JA-Ile, a hormone linked with salt adaptation, is accompanied by more robust redox homeostasis in a different organelle, the mitochondrion, indicates that cross-talk between peroxisome and mitochondrion is a crucial factor for efficient adaptation to salt stress.

Abbreviations: AOC, allen oxide cyclase; AOS, allen oxide synthase; BY-2, *Nicotiana tabacum* L., cv. Bright Yellow 2; COI1, coronatine insensitive 1; CSC, cysteine synthase complex; GFP, green fluorescent protein; JA, jasmonic acid; JA-Ile, jasmonoyl isoleucine; MnSOD, manganese superoxide dismutase; MeJA, methyl jasmonate; OPDA, 12-oxo-phytodienoic acid; OPR7, 12-oxo-phytodienoic acid reductase 7; OsOPR7, *Oryza sativa* 12-oxo-phytodienoic acid reductase 7; SAT, serine acetyltransferase.

* Corresponding authors at: Molecular Cell Biology, Botanical Institute, Karlsruhe Institute of Technology, Fritz-Haber-Weg 4, D-76131, Germany.
E-mail addresses: kinfe_michael2006@yahoo.com (K.G. Asfaw), peter.nick@kit.edu (P. Nick).

https://doi.org/10.1016/j.plantsci.2021.111156
Received 27 August 2021; Received in revised form 1 December 2021; Accepted 11 December 2021
Available online 13 December 2021

1. Introduction

Salinity is one of the most serious and devastating abiotic stress factors that threatens global agriculture. About 20 % of cultivated land worldwide have been affected by salinity and the value is increasing at an alarming rate [1,2]. Salinity severely affects plant growth and development in a complex manner through its osmotic, ionic and oxidative components [3]. However, since salt stress had accompanied plants throughout their entire evolution, plants have developed various mechanisms to cope with its detrimental effects (reviewed in [2,4]). Among the regulatory factors that orchestrate salt adaptation, several phytohormones have been shown to play a central role (for review see [5]). Among the hormonal pathways, jasmonate signalling is crucial for the response to salinity. Here, both, the precursor 12-oxo-phytodenoic acid (OPDA), as well as the final product of the pathway, jasmonoyl isoleucine (JA-Ile), are actively participating in signalling but triggering different outputs, depending on their respective temporal patterns (reviewed in [6]). While OPDA is usually converted rapidly to the precursors of JA-Ile, it may, if accumulating, trigger a separate signalling, culminating in salinity-induced necrosis [7]. Instead, JA-Ile initiates cellular adaptation (it refers to the plethora of responses described in this work, where the cells, by adjusting gene expression, acquire a more robust redox homeostasis and, thus, physiological resilience) to salinity. This adaptation is strongly dependent on the time course – a swift and transient activation of JA-Ile signalling is mandatory for cellular adaptation, while constitutive activation results in necrosis [6]. These findings indicate that the biosynthesis of jasmonates must be exactly tuned to achieve efficient adaptation.

Biosynthesis of JA (for a recent review refer to [8]) is triggered by external stimuli and initiated by the release of α-linolenic acid (a 18:3 fatty acid) from chloroplast membranes by type A phospholipase 1. Upon the release of α-linolenic acid into the stroma, molecular oxygen is incorporated by a lipoxygenase to form 13S-hydroperoxy-(9Z, 11E, 15)-octadecatrienoic acid (13-HPOT), which is further metabolised by different members of the CYP74 cytochrome P_{450} family into different products. One of these members, CYP74A, or allene oxide synthase (AOS), can oxidise 13-HPOT to the chemically unstable allene oxide. Subsequently, the allene oxide is converted by allene oxide cyclase (AOC) into OPDA. which is exported from the plastid and imported to the peroxisome, which is at least in part mediated by the ATP binding-cassette transporter COMATOSE. In the peroxisome, OPDA is reduced by 12-oxo-phytodienoic acid reductase (OPR) to 3-oxo-2-(2′(Z)-pentenyl)-cyclopentane-1 octanoic acid (OPC-8:0), and then transformed into (+)-7-*iso*-JA. Additional three β-oxidation cycles are catalysed by acyl-CoA oxidase, a multifunctional protein complex comprising an enoyl-CoA hydratase, a hydroxy-acyl-CoA dehydrogenase, and 1−3-keto-acyl-CoA thiolase. The resulting cis-7-*iso*-jasmonic acid [(+) -7-*iso*-JA] is then released from the peroxisome to the cytoplasm. Here, it can either be methylated by the JA-carboxyl methyltransferase into the volatile methyl jasmonate (MeJA) or conjugated to L-isoleucine by the enzyme jasmonate amino acid synthetase which is encoded by the JA resistant 1 (*JAR1*) gene. This conjugated JA-Ile represents the bioactive form of the hormone.

In jasmonate signalling, the activation of jasmonate dependent responses requires ubiquitin-mediated degradation of the transcriptional repressor, JASMONATE ZIM/tify-DOMAIN (JAZ/TIFY) proteins (reviewed in [9]), that actively suppress the transcriptional activator JASMONATE INSENSITIVE 1/MYC2 [10]. However, when JA-Ile forms in response to biotic and abiotic stress or during development, it will bind to its cognate receptor Coronatine Insensitive 1 (COI1). This will lead to ubiquitination and degradation of JAZ/TIFY proteins through the 26S proteasome, which will release JIN1/MYC2, along with additional transcription factors, from repression. Thus, it is the de-repressed JIN1/MYC2 that triggers the transcription of JA-responsive genes [9]. Among these genes are the JAZ /TIFY repressors themselves [10], such that the newly synthesized JAZ/TIFY proteins will restore the repression and shut off JA signalling again (reviewed in [11]). This negative feedback mechanism ensures that a jasmonate signal remains transient, which is crucial to deploy efficient adaptation against different stresses, among them salinity (reviewed in [6]).

In addition to their well-known role in the response to herbivory, jasmonates are important key regulators for plant adaptation to abiotic stress including drought and salt stress (reviewed in [12]). Here, not only JA-Ile, but also its precursor OPDA is an important signal activating partially different sets of genes [13] and, therefore, obviously conveys a different function during the response to salinity. In fact, OPDA has been found to control redox homeostasis in chloroplasts through regulating sulphur metabolism [14]. In rice, salt stress leads to a strong accumulation of OPDA, correlating with necrosis, while two allene oxide cyclase loss-of-function mutants that cannot form OPDA, cope better with salt stress [7]. Note that salt necrosis triggered by OPDA could be of adaptive value on the level of the entire plant: By their commitment for necrosis, especially older leaves can sequester salt from the vital meristems that will be able to generate new organs, once the salt-stress episode has passed [15]. Thus, it seems that the steady-state level of OPDA represents something like an important switch: When OPDA efficiently converts to JA-Ile, cellular adaptation should result, if it accumulates, programmed cell death should be favoured. This decision assigns a central role to OPDA reductases.

Based on their substrate preference, the OPRs are categorised into two subgroups [16–20]. Subgroup OPRI preferentially reduce (-)-cis-OPDA, if tested *in vitro* [18,17–20]. Nevertheless, their preferential substrate *in vivo* has remained unknown, and to what extent they participate in JA biosynthesis and signalling is far from clear either [21]. In contrast, the subgroup OPRII can reduce all the four OPDA isomers [(cis-(+), cis-(-), trans-(+) and trans-(-)]; however, *in planta*, type-II OPRs preferentially reduce cis-(+)-OPDA to OPC 8:0, and, therefore, are thought to be responsible for the biosynthesis of JA [17]. Rice OPR7 (OsOPR7) belongs to these type-II OPRs and, thus, represents the rice homologue responsible for JA biosynthesis. Also the localisation of OsOPR7 is in the peroxisomes, i.e. in the organelle, where the downstream reduction of OPDA in JA biosynthesis occurs [20], is consistent with the notion of homology.

The cross talk between organelles is, thus, relevant for efficient cellular responses to stress. In fact, peroxisomes communicate and associate with other organelles such as lipid bodies, chloroplasts, and mitochondria to carry out their multi-faceted functions in cells such as photorespiration, lipid mobilisation and redox metabolism [22]. Plant peroxisomes are often observed adjacent to chloroplasts and mitochondria [23–26], and even can form extensions, called peroxules [27]. Peroxules are thought to facilitate the exchange of metabolites and proteins with other organelles, such as mitochondria, plastids, or ER, especially in response to reactive oxygen species (ROS) that are generated in peroxisomes, chloroplasts and mitochondria under the influence of environmental stress [27,28]. These ROS signals from the three organelles are proposed to interact in the cytoplasm and to convey a signal to the nucleus deploying appropriate expression of nuclear genes (for reviews see [26,29,30]). However, to what extent the retrograde pathways from peroxisomes, chloroplasts and mitochondria connect to one another and which molecular mechanisms are involved, is far from understood [26]. For retrograde signalling from light-stressed plastids, first molecular candidates have emerged that are also interacting with jasmonate synthesis [31]. For mitochondrial retrograde signalling, transcription perturbed oxidative balance will result in the cleavage of specific transcription factors that are tethered at the adjacent ER, such that a fragment with transcriptional activity is released and moves into the nucleus [32]. However, mitochondria and chloroplasts do not only interact with peroxisomes and nucleus, but also among themselves, and this is in both directions. So far, two mechanisms can explain this phenomenon. On the one hand, the respective retrograde signalling can share common factors, such as the cyclin-dependent kinase E1 (reviewed in [33]), on the other hand, some proteins show dual targeting to both

organs which results in coupling the organelles [34].

In our previous work, we have shown that Plant PeptoQ, a cell penetrating peptoid with a mitochondria-targeting motif and endowed with a semiquinone moiety mimetic of coenzyme Q10, was rapidly and efficiently targeted to the mitochondria of walled tobacco BY-2 cells [35], which conferred improved resilience to salt stress. Subsequently, we could show that this mitigation was caused by a modulation of retrograde signalling culminating in higher expression of the mitochondrial superoxide dismutase [36]. However, we also observed that the Plant PeptoQ significantly increased the steady-state levels of OPDA, although OPDA is synthetised in a different organelle, the plastid. This indicates that the redox homeostasis in the mitochondria conveys a signal either to the plastid, where OPDA accumulates, or to the peroxisome, where OPDA converts further. If the mitochondrial signal targets to the peroxisome, overexpression of *OsOPR7* should modulate this signal. To test this implication, we overexpressed the *OsOPR7* gene from rice in tobacco BY-2 cells. We show that the OsOPR7-GFP protein is correctly localised in peroxisomes. We then compared the salt-stress responses of the *OsOPR7* overexpressor to those of non-transformed cells, where Plant PeptoQ buffers mitochondrial redox homeostasis, and we show that overexpression of *OsOPR7* and addition of Plant PeptoQ produce similar patterns. If the Plant PeptoQ and the overexpressed enzyme were addressing non-related cellular targets, their combination should act additively. We do not observe this - in some cases they even act antagonistically. We interpret our data using a model, where the organelles endowed with oxidative metabolism (mitochondria, peroxisomes, and plastid) communicate with each other.

2. Results

2.1. OsOPR7-GFP is localised in the peroxisomes

To identify the subcellular localisation, we introduced a GFP-fusion construct of the *OsOPR7* into tobacco BY-2 cells under control of the constitutive CaMV-35S promoter in a binary vector using *Agrobacterium* transformation and selection on hygromycin. The resulting transformants displayed a punctate signal distributed all over the cytoplasm (Fig. 1A, left-hand image), consistent with the expected peroxisomal localisation of this protein. To verify this supposition, these *OsOPR7*-GFP cells were transformed additionally with the peroxisomal signal peptide PTS1 fused to the red fluorescent protein mCherry [37], using a transient, *Agrobacterium* based protocol [38]. The PTS1-mCherry marker (Fig. 1A, central image) visualised the same punctate structures as those seen with OsOPR7-GFP, and both signals colocalised significantly (Fig. 1A, right-hand image). In contrast, when the *OsOPR7*-GFP overexpressor cells were labelled with rhodamine labelled Plant PeptoQ (Fig. 1B, central image), the two signals did not show any colocalisation (Fig. 1B, right-hand image). Thus, the overexpressed GFP-fusion of OsOPR7 was correctly localised in the peroxisomes, supporting the notion that the fusion protein is functional.

2.2. OsOPR7 overexpressor cells are more resilient against salt stress

Cell proliferation belongs to the most sensitive physiological markers for salt stress. We followed, therefore the progress of cell density over time, either in the absence of salt stress, under moderate salt stress (75 mM NaCl), or under severe salt stress (150 mM NaCl), comparing the *OsOPR7* overexpressor (Fig. 2B) to non-transformed WT BY-2 cells (Fig. 2A). In the absence of salt stress, both cell lines proliferated vigorously. For moderate salt stress (75 mM NaCl), proliferation became inhibited, however, the inhibition was far less pronounced in the *OsOPR7* overexpressor. For instance, 72 h after the onset of salinity stress, cell density in the non-transformed WT BY-2 cells had dropped by 60 % as compared to the non-stressed control, while in the *OsOPR7* strain, this reduction was only 37 %. For severe salt stress (150 mM NaCl), proliferation was strongly suppressed in both lines, but the residual activity in the *OsOPR7* overexpressor (17 % at 96 h) was still higher than that seen in the non-transformed WT BY-2 (only 8% at 96 h). The higher resilience of the *OsOPR7* overexpressor was also evident, when we estimated doubling times from the time course of cells proliferation using an exponential growth model (Fig.2C). Here, doubling time in the non-transformed WT-BY2 increased dramatically, when salinity increased from 0 to 150 mM NaCl. At moderate salt stress, the doubling time had almost doubled (39 h) as compared to the control, and at severe salt stress, a value of 330 h reports that these cells have ceased to proliferate. In contrast, the *OsOPR7* overexpressor doubled every 28 h under moderate salt stress (almost preserving the proliferation activity seen in the control). Even under severe salt stress, it was

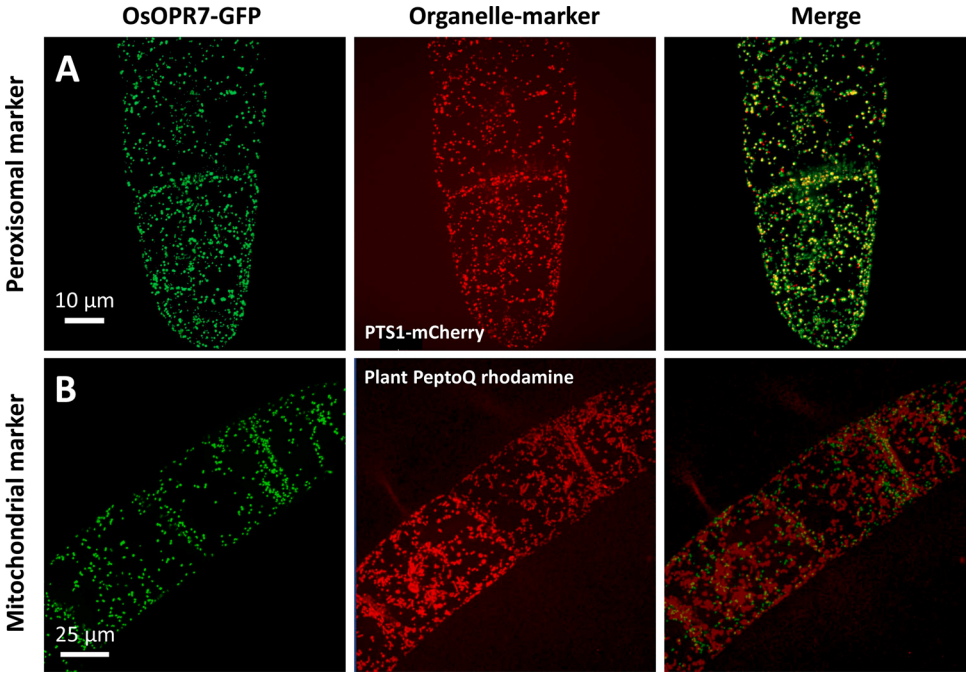

Fig. 1. Peroxisomal localization and non-mitochondrial localization of OsOPR7 protein in *OsOPR7* overexpressor tobacco BY-2 cells assessed at day 3 (**A, B**). The *OsOPR7*-GFP transformed suspension BY-2 cells were co-transformed with agrobacterium containing PTS1-mCherry plasmid. Grown on solid Paul's medium for 3 days, and then followed by spinning disc confocal microscopy making use of the red fluorescent signal from PTS1-mCherry (**A** center), and the green, fluorescent signal from GFP (**A** left). The merge of the two channels shown in (**A** right) shows the close overlap of both signals. Similarly, the non-mitochondrial localization of OsOPR7 protein is evident from the lack of colocalisation (**B** right) between the red fluorescence signal from rhodamine labelled Plant PeptoQ (**B** center) and the green fluorescence signal from GFP (**B** left). Confocal sections recorded in the mid-plane from representative cells recorded at constant laser power and exposure time are shown. (For interpretation of the references to colour in this figure legend, the reader is referred to the web version of this article).

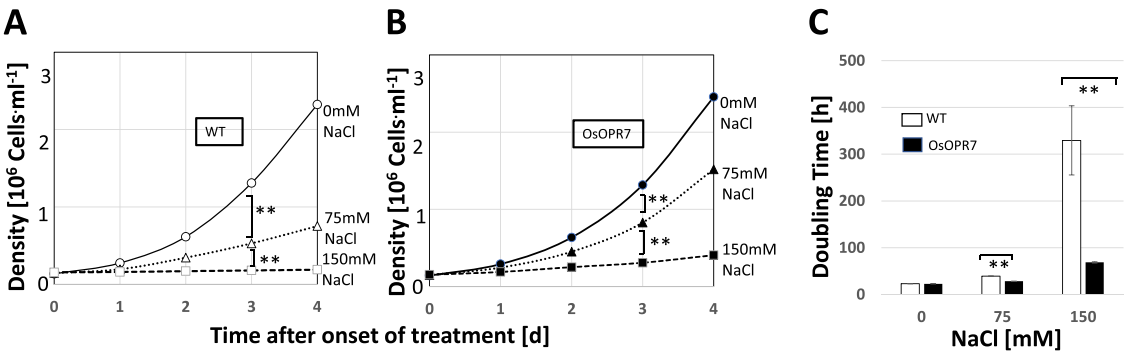

Fig. 2. Effect of the overexpression of *OsOPR7* gene on salt-induced inhibition of cell proliferation in tobacco BY-2 cells. Time courses of cell density in the absence of salt stress (0 mM NaCl, white and black circles), under moderate (75 mM NaCl, white and black triangles), and under stringent (150 mM NaCl, white and black squares) salt stress in WT (**A**) and *OsOPR7* overexpressor (**B**) BY-2 cells. **C** Doubling time estimated from the time constant of exponential growth over the concentration of NaCl, WT (open bars) and *OsOPR7* overexpressor (filled bars) BY-2 cells. Data represent mean values and standard errors of three independent experimental series. ** indicate differences significant at $P \leq 0.01$ based on a Student's *t*-test.

able to sustain a doubling time of 69 h (around three times slower than in the control, but five times faster than the non-transformed WT BY-2 under these conditions). Thus, the sensitivity of doubling against salt dropped significantly in the *OsOPR7* overexpressor.

As cells enlarge their central vacuole during expansion phase between day 3 and day 7 after subcultivation, we asked whether mitigation of salt stress would improve cell expansion (Fig.3A). In non-transformed WT BY-2 cells, already for moderate salt stress (75 mM NaCl), relative growth rate decreased profoundly with less than 30 % residual growth as compared to the untreated control. The value became even negative for stringent salt stress (150 mM NaCl), which implies the cells shrank. This was perhaps due to the osmotic potential in the protoplast being less negative than that of the medium. Under control conditions, the *OsOPR7* overexpressor only produced around half of the cell expansion seen in the non-transformed wild type. However, this expansion remained stable for moderate salt stress (75 mM NaCl), which significantly excelled the expansion of the non-transformed wild type. Even under severe salt stress (150 mM NaCl), a residual expansion of about 24 % of the control level remained, contrasting sharply with the severe shrinkage seen in the non-transformed wild type. Thus, compared to cell proliferation (Figs. 2A, **B**), the stress compensation seen for cell expansion (Fig. 3A), was even more pronounced.

The terminal consequence of salt-induced arrest is cell death. We followed the time course of salt-induced mortality using the Evans Blue Dye Exclusion assay over four days (**Suppl. Fig. S1**). In non-transformed cells, at moderate salt stress (75 mM NaCl), mortality sharply increased significantly to more than 40 % over 24 h, but it decreased during later incubation times reaching 20 % at 96 h (**Suppl. Fig. S1A**). Since dead cells are rapidly decaying to debris in a suspension culture under continuous shaking, the values measured by Evans Blue represent steady-state estimations of mortality. The ongoing proliferation of surviving cells will therefore cause a decrease of steady-state mortality. Here, there is of course no resurrection of cells, but dead cells in suspension decay to debris (also due to the shear stress from shaking) and, thus, disappear from the population, while the surviving cells are adapted. The mortality score is, therefore, representing a steady-state between decay and cell death. The *OsOPR7* overexpressor produced a similar temporal pattern, albeit at a slightly but significantly reduced amplitude. At moderate salt stress (75 mM NaCl), the maximum cell mortality at 24 h was 38 % and it dropped to 15 % at 96 h. This implies that more cells were able to return to viability through the elapse of time as compared to the case in salt stressed WT BY-2 cells (**Suppl. Fig. S1A**). At stringent salt stress (150 mM NaCl), no residual proliferation was seen (**Suppl. Fig. S1B**), such that mortality remained high after the initial sharp increase (up to 80 % in the non-transformed wild type). However, again, we found the amplitude in the *OsOPR7* overexpressor to be significantly lower. When we measured a dose-response of mortality scored 24 h after the onset of salt stress (Fig. 3B), we saw a significant shift to higher concentrations in the *OsOPR7* overexpressor. The LD_{50} value determined for the non-transformed wild type was at 92 mM NaCl, while for the *OsOPR7* overexpressor this value was significantly higher (106 mM NaCl).

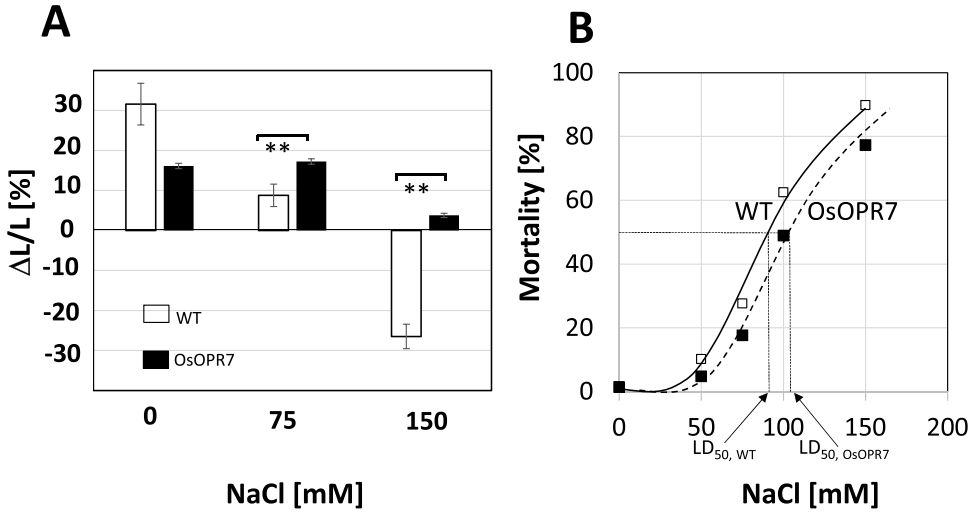

Fig. 3. Effect of *OsOPR7* overexpression on salt-induced inhibition of cell expansion and salt induced mortality in tobacco BY-2 cells. **A** relative elongation during the expansion phase (days 3 to 7 after subcultivation) in control (0 mM NaCl), under moderate (75 mM NaCl), and under stringent (150 mM NaCl) salt stressed WT (open bars) and *OsOPR7* overexpressor (filled bars) BY-2 cells. **B** In comparison with the *OsOPR7* overexpressor, the LD_{50} in the WT BY-2 cells, occurs significantly at a lower NaCl concentration. Data represent mean values and standard errors of three independent experimental series. ** indicate differences significant at $P \leq 0.01$ based on a Student's *t*-test.

In summary, *OsOPR7* overexpression lead to an improved resilience of tobacco BY-2 cells against salinity stress. For moderate salt stress (75 mM NaCl), cell expansion was fully preserved, and even proliferation and viability were still partially retained. A partial, but significant mitigation was present even at stringent salt stress (150 mM NaCl). Thus, with respect to physiological parameters, overexpression of *OsOPR7* shifts cells of tobacco (an extreme glycophyte) to tolerance levels of marginal halophytes, such as barely and date palm [39].

2.3. *OsOPR7 overexpressor cells are superior in maintaining superoxide homeostasis under salt stress*

The higher resilience of proliferation, expansion, and viability under salt stress in the *OsOPR7* overexpressor might either derive from a reduced uptake of sodium ions. Alternatively, it might derive from a more robust metabolic buffering, especially of the oxidative processes in the mitochondria (since tobacco BY-2 cells lack chlorophyll, oxidative photophosphorylation, in green leaves which is the major source of reactive oxygen species, does not play a role).

To distinguish between the two mechanisms, we first measured the content of sodium and potassium after treatment with 0, 75, and 150 mM NaCl in both, WT and *OsOPR7* overexpressor (**Suppl. Fig. S2**). As expected, salt stress caused a dose dependent increase in the content of sodium ions (**Suppl. Fig. S2A**). The increase was quite strong and not alleviated by *OsOPR7* overexpression. There was a significant decrease in potassium ions following the uptake of sodium ion (**Suppl. Fig. S2B**). Despite the fact that sodium uptake was doubled at stringent salt stress (150 mM NaCl), as compared to moderate salt stress (75 mM NaCl), the decrease in potassium ion was already saturated for 75 mM NaCl and was not accentuated further for stringent salt stress (150 mM NaCl). Similar to the situation with sodium ion, *OsOPR7* overexpression had no significant effect on the uptake of potassium ions. Thus, under salt stress, ionic balance was strongly perturbed, and did not show any significant alleviation in the *OsOPR7* overexpressor. Thus, we can rule out reduced ion uptake as mechanism behind the improved salt tolerance of the *OsOPR7* overexpressor.

We wondered, therefore, whether the superior resilience of the *OsOPR7* overexpressor correlates with a superior oxidative homeostasis. One readout for oxidative degradation of membranes is the level of lipid peroxidation reported by the product malondialdehyde (MDA [40]). When we followed MDA levels in response to salt stress in cells at the onset of expansion (day 4 after subcultivation), we observed a dose-dependent increase in the WT. This increase was already manifest at 1 h after the onset of salt stress (Fig. 4A). In case of stringent salt stress (150 mM NaCl), this value had increased further at 4 h after the onset of salt stress. Here, the MDA level had more than doubled as compared to the un-stressed control (Fig. 4B), while for moderate salt stress the MDA level remained at the value seen after 1 h. In the *OsOPR7* overexpressor, the salt-induced increase of MDA steady-state levels was absent for moderate salt stress (Figs. 4**A, B**). Even under stringent salt stress (150 mM NaCl), the MDA level where significantly lower as compared to the WT and equaled the values seen in the WT seen for moderate salt stress (75 mM NaCl). Thus, with respect to MDA levels, the *OsOPR7* overexpressor was roughly twice as tolerant as compared to the WT.

To understand the relation of the observed lipid peroxidation (measured by MDA) with the reactive oxygen species (ROS), we determined the steady-state levels of superoxide (**Suppl. Fig. S3A**) along with the activity of superoxide dismutase (Fig. 4C). In the wild type, steady-state levels of superoxide decreased significantly with increasing salinity. Already moderate salinity (75 mM NaCl) reduced enzymatic activity by more than half as compared to the control (Fig. 4C). Concomitantly with this decrease of superoxide dismutase, superoxide steady-state levels rose (**Suppl. Fig. S3A**), albeit the variability of the values was relatively high, such that the substantial difference of the mean was not significant due to large standard errors. In contrast, the *OsOPR7* overexpressor maintained a high and unchanged activity of

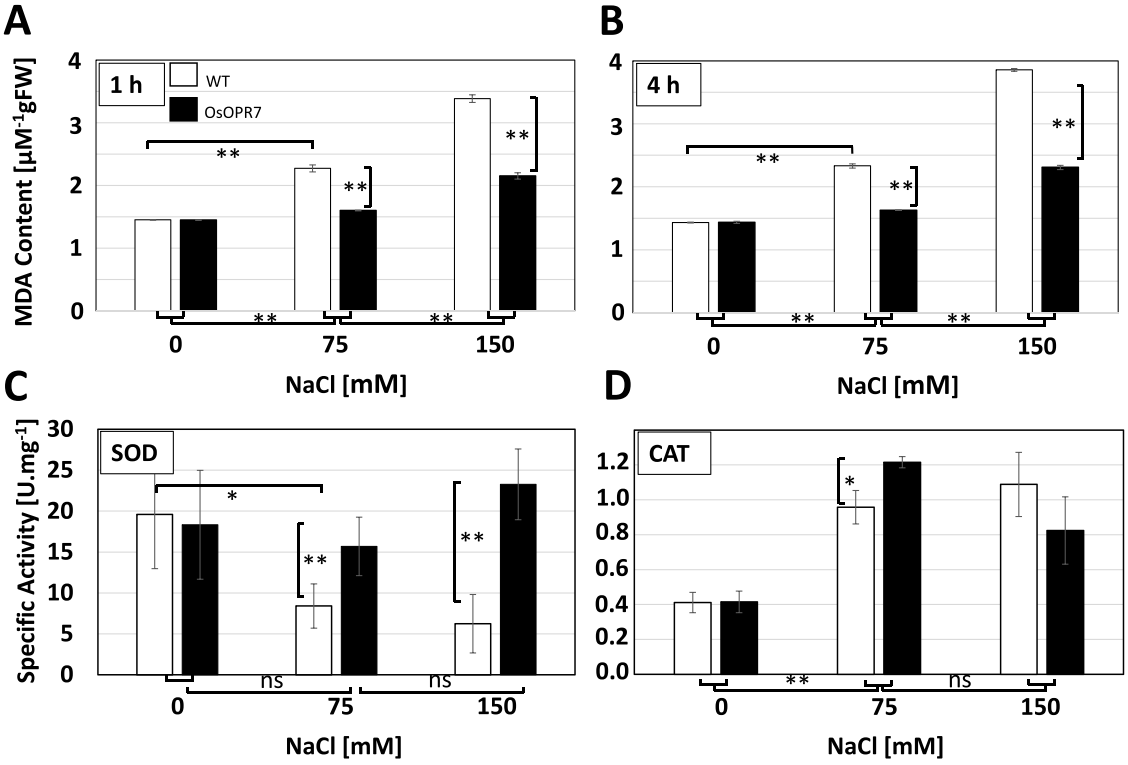

Fig. 4. Effect of *OsOPR7* overexpression on oxidative balance. **A, B** Content of malone dialdehyde (MDA) under moderate (75 mM NaCl), and stringent (150 mM NaCl) salt stress, measured 1 (**A**) and 4 h (**B**) after the onset of the respective treatment in WT (open bars) and *OsOPR7* overexpressor (filled bars) BY-2 cells. **C, D** Effect of moderate (75 mM NaCl) and stringent (150 mM NaCl) salt stress on SOD and CAT activities. Data represent mean values and standard errors of three independent experimental series. ** indicate differences significant at $P \leq 0.01$, *at $P \leq 0.05$ based on a Student's *t*-test.

SOD (Fig. 4C), which correlated with a significant decrease of superoxide steady state levels (**Suppl. Fig. S3A**). Thus, overexpression of *OsOPR7* leads to a more resilient superoxide dismutase activity under salt stress resulting in reduced steady-state levels of superoxide.

Along the same line, we measured the steady-state levels of hydrogen peroxide (**Suppl. Fig. S3B**) along with the activity of catalase (Fig. 4D). In the wild type, steady-state levels of hydrogen peroxide increased around twofold with increasing salinity, which already had reached a plateau at 75 mM NaCl. In parallel, catalase activity increased as well. For the *OsOPR7* overexpressor, the pattern was identical, except a significant increase in peroxide ground levels by around 50 % (although catalase activity was identical to the wild type). Likewise, at 75 mM NaCl, catalase activity was mildly (by around 20 %), but significantly increased over the activity in the wild type. Thus, in comparison to the superoxide status, the peroxide status does not reveal a tight link with the mitigating effect of *OsOPR7* overexpression.

2.4. OsOPR7 overexpressor cells sustain higher transcript levels for mitochondrial SOD

The *OsOPR7* overexpressor sustained higher activities of SOD under salt stress and was able to contain the accumulation of superoxide. We asked, therefore, whether this pattern would become manifest on the level of steady-state transcript levels for the mitochondrial *MnSOD*. In the wild type, transcript levels at 1 h (Fig. 5A) increased almost 20-fold as compared to the control for moderate salt stress but dropped back to the resting levels for stringent salt stress. Later, at 3 h (Fig. 5B), both salinity levels induced around 10-fold more transcripts as compared to the untreated control. These increased steady-state transcript levels did not correlate with the enzymatic activity (Fig. 4C) that dropped with increasing concentration of NaCl. Thus, the increased *SOD* transcripts do not cause a better oxidative balance. For the *OsOPR7* overexpressor, the resting levels of *MnSOD* transcripts were more than an order of magnitude higher and persisted at this level under salt stress, if scored at 1 h (Fig. 5A). They approximated the levels seen in the wild type, if scored at 3 h (Fig. 5B). This correlates with a persisting enzymatic activity under salt stress (Fig. 4C). Thus, the initially elevated level of *MnSOD* transcripts heralds the more persistent oxidative balance under salt stress.

The increase of steady-state transcript levels seemed to be specific for *MnSOD* as seen from a comparative study with nine genes linked with different aspects of salinity signalling or adaptation (Fig. 5C, **Suppl. Fig. S4**). Transcripts for *MnSOD* probed redox homeostasis (*MnSOD*). The genes for *SOS1* (a transporter extruding sodium to the apoplast), *NHX1* (a transporter sequestering sodium in the vacuole) and *SKOR* (a channel balancing potassium–sodium homeostasis) represented ion channels. The genes for *SOS3* (transducing calcium upon the activity of *SOS1*) and *STL1* (a phosphatase regulating potassium–sodium homeostasis) reported regulation of ion channels. The genes for *OsOPR7* itself, and *JAZ3* (a jasmonate response gene related to salinity) probed the jasmonate status. While the overall expression of these genes was quite similar between WT and overexpressor, a few differences emerged. *OPR7* itself displayed transcript levels that were strongly (around 2500-fold) elevated in the *OsOPR7* overexpressor (Fig. 5C, **Suppl. Fig. S4F**). This is an expected outcome from overexpression of this gene under control of the strong and constitutive CaMV-35S promoter. In the absence of salt stress, the regulator *SOS3* was significantly (by around fourfold) downregulated in the *OsOPR7* overexpressor (Fig. 5C, **Suppl. Fig. S4E**). Likewise, the transcripts for *NAC* were significantly lower in the *OsOPR7* overexpressor and remained so under salt stress (Fig. 5C, **Suppl. Fig. S4H**). Thus, elevated expression of *OsOPR7* correlates with elevated steady-state levels of *MnSOD*, while transcripts for *SOS3* and *NAC* are lower.

2.5. OsOPR7 overexpressor cells shift jasmonate metabolism towards OPDA

Salt stress leads to activation of jasmonate synthesis and signalling, which improves adaptation, if appropriately down-modulated, but can initiate salinity-induced necrosis, if constitutively active [6]. Therefore, we compared the levels of the precursor OPDA, JA, and the final product JA-Ile in salt stressed WT and *OsOPR7* overexpressor BY-2 cells after 1 and 3 h of salt stress. While JA was not detectable in none of the samples (indicative of a fast conversion into the terminal product JA-Ile), OPDA and JA-Ile accumulated to measurable amounts (Fig. 6). In the *OsOPR7* overexpressor, the steady-state levels of OPDA were higher than in the WT (Fig. 6A). This difference was already present without salt stress, and even increased mildly during salt stress. However, theoretically, as the level of OPR activity is high in the OsOPR7 overexpressor, the steady-state levels of OPDA should be lower than in the WT because OPDA is converted on the path to JA by OsOPR7 enzyme. In contrast, the steady-state levels of JA-Ile were not significantly different between the two cell lines (Fig. 6B). When the WT was exposed to moderate salt stress (75 mM NaCl), the molar ratio of JA-Ile over OPDA increased over time (Fig. 6C). This increase was yet not detectable at 1 h, but had reached a surplus of around 1/3 at 3 h after the onset of salt stress. This increase was absent in the *OsOPR7* overexpressor. Even under severe salt stress (150 mM NaCl), where the JA-Ile to OPDA ratio in the wild type had returned to the resting level, this ratio was significantly higher in the wild type, because the value in the *OsOPR7* overexpressor had decreased significantly in comparison to the resting level. Thus, although, *OPR7* transcripts have increased strongly, by more than 2000-fold (Fig. 5C, **Suppl. Fig. S4F**) in the *OsOPR7* overexpressor, this does not lead to a

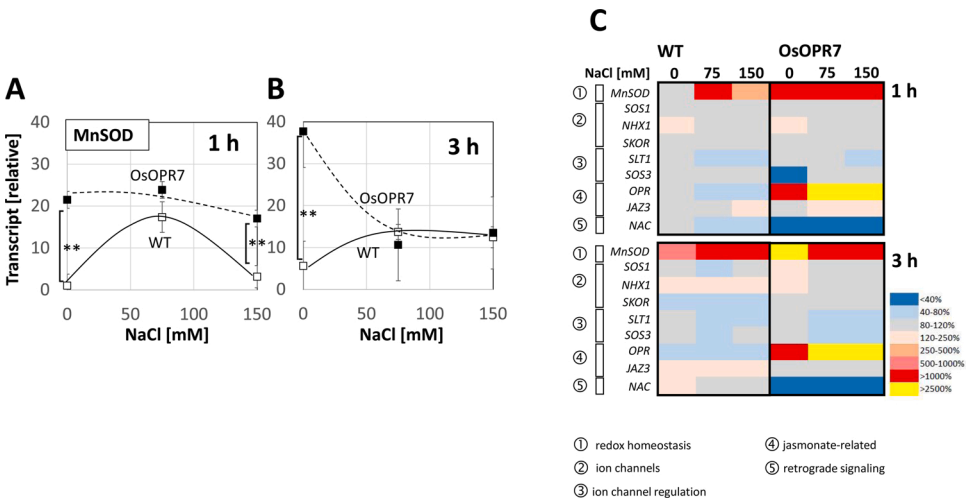

Fig. 5. The relative expression of manganese superoxide dismutase (*MnSOD*), mitochondrial gene, at earlier (1 h) (**A**) and later (3 h) (**B**) time points in salt stressed WT (black curve) and *OsOPR7* overexpressor (broken curve) BY-2 cells. **C** The expression of all the other salt-stress related genes in salt stressed WT and *OsOPR7* overexpressor BY-2 cells at 1 and 3 h. Data represent mean values and standard errors of three independent experimental series. ** indicate differences significant at $P \leq 0.01$ based on a Student's *t*-test.

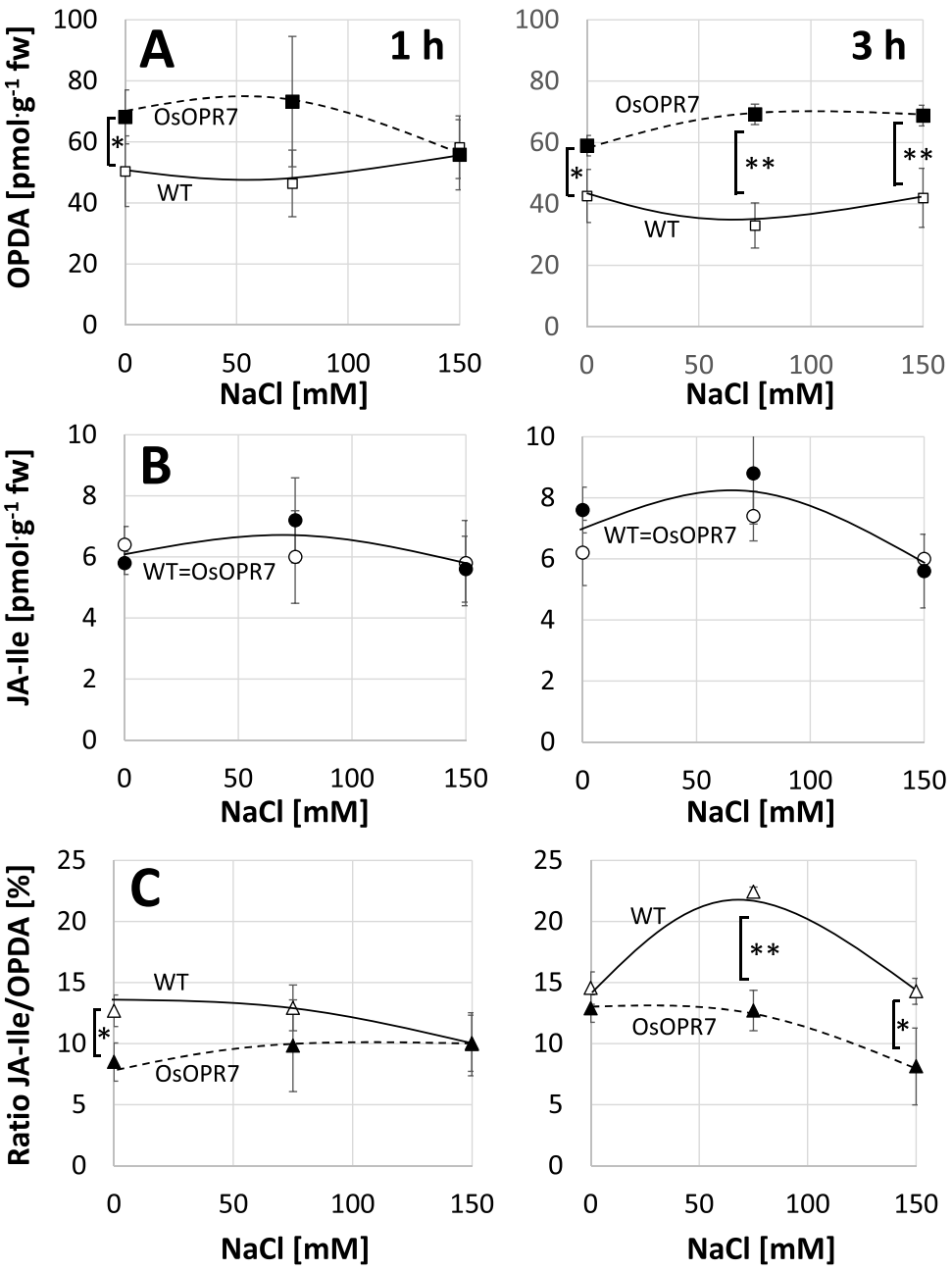

Fig. 6. Effect of salt stress on 12-oxo-phytodienoic acid (12-OPDA) and Jasmonic acid-isoleucine (JA-Ile) level as well as JA-Ile/OPDA (%). **A** The level of 12-OPDA in WT (grey curve) and *OsOPR7* overexpressor (broken curve) BY-2 cells. **B** The level of JA-Ile in WT and *OsOPR7* overexpressor (grey curve, both) BY-2 cells. **C** JA-Ile/OPDA (%) in WT (grey curve) and *OsOPR7* overexpressor (broken curve) BY-2 cells. Data represent mean values and standard errors of three independent experimental series. ** indicate differences significant at $P \leq 0.01$, *at $P \leq 0.01$ based on a Student's *t*-test.

reduced steady state level of OPDA, the substrate of this enzyme. Instead, there is a surplus of OPDA relative to the final product of the pathway, JA-Ile.

2.6. Plant PeptoQ and OsOPR7 do not act additively, although they act in different locations

Several aspects of OsOPR7 were congruent with the effect observed earlier after treatment with Plant PeptoQ, a peptoid with antioxidant activity that rapidly accumulates in mitochondria [35]. These include the mitigation of salt-induced mortality, and accumulation of superoxide, anticipative upregulation of mitochondrial *MnSOD* transcripts prior to salt stress, or the increased steady-state levels of OPDA over JA-Ile. This overlap of very specific features contrasts with the localisation in different organelles – Plant PeptoQ acts in mitochondria, while OPR7 acts in peroxisomes. If their mitigating effect would stem from different and unrelated causes, their combination should lead to an additive effect. We, therefore, assessed the response of the *OsOPR7* overexpressor to Plant PeptoQ.

We, first, determined the steady-state transcript levels of *MnSOD* (Fig. 7A, **B**). In the wild type, in absence of Plant PeptoQ these increased in response to salt stress (more rapidly for 75 mM NaCl, more slowly for 150 mM NaCl). Pretreatment with Plant PeptoQ increased the resting levels (0 mM NaCl) within 1 h by a factor of 10 compared to the situation without Plant PeptoQ and salt stress (Fig. 7A). At 3 h (Fig. 7B), the levels had increased further by additional twofold. Also in the *OsOPR7* overexpressor without Plant PeptoQ, the resting levels of *MnSOD* transcripts were high (around 20-fold over the wild type at 1 h) and remained high under salt stress. At a later time (3 h), they were high in the absence of salt stress, but dropped to the levels in the wild type under salt stress. Thus, treatment of the wild type with Plant PeptoQ, or overexpression of *OsOPR7* had a similar effect upon *MnSOD* transcripts. A combination treatment was not giving further improvement, if assessed at 1 h (Fig. 7A). Here, the resting levels for *MnSOD* transcripts in Plant PeptoQ-

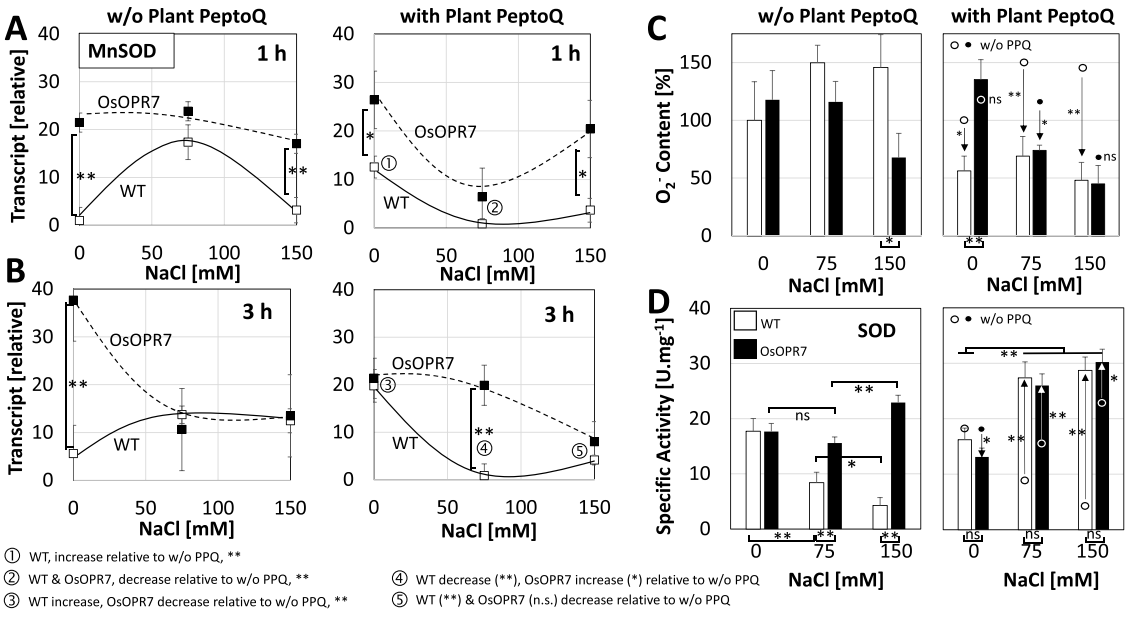

Fig. 7. The relative expression of manganese superoxide dismutase (*MnSOD*), mitochondrial gene, in salt stressed WT (grey curve) and *OsOPR7* overexpressor (broken curve) BY-2 cells in the absence and presence of Plant PeptoQ pretreatment at earlier (1 h) (**A,** left, right) and later (3 h) (**B** left, right) time points, respectively. Superoxide level in the absence (**C** left) and presence (**C** right) Plant PeptoQ pretreatment. Superoxide dismutase (SOD) activity in the absence (**D** left) and the presence (**D** right) Plant PeptoQ pretreatment. Data represent mean values and standard errors of three independent experimental series. ** indicate differences significant at $P \leq 0.01$, * at $P \leq 0.05$ based on a Student's *t*-test.

treated *OsOPR7* cells was only slightly (and not significantly) higher than in *OsOPR7* cells without Plant PeptoQ. At 75 mM NaCl, they even dropped to less than half of the value seen without Plant PeptoQ, i.e. the Plant PeptoQ treatment acted antagonistically to the effect of *OsOPR7* overexpression. Antagonistic interaction was also prevailing at 3 h (Fig. 7B). Here, the strong excess of *MnSOD* transcripts seen for the absence of Plant PeptoQ in *OsOPR7* overexpressor cells over the wild type, was completely gone – in presence of the Plant PeptoQ the steady state levels were the same in both cell lines, because they had increased in the wild type, but decreased in the *OsOPR7* overexpressor. However, under moderate salt stress (75 mM NaCl), Plant PeptoQ, treatment was able to sustain the *MnSOD* transcript levels that dropped strongly in the wild type. Summarising, the interaction of *OsOPR7* overexpression and Plant PeptoQ was clearly not additive, in some cases even antagonistic.

Although the *MnSOD* transcript levels allow drawing conclusions on retrograde signalling between mitochondria and nuclear genome (where the *MnSOD* gene is located), they neither predict the activity of the encode enzyme, nor the dissipation of superoxide in a straightforward manner. We, therefore, measured superoxide content (Fig. 7C) and SOD enzyme activity (Fig. 7D) in wild type and *OsOPR7* overexpressor under salt stress either without or with Plant PeptoQ pretreatment. While in the absence of the Plant PeptoQ, the superoxide steady-state levels of the wild type were progressively increasing (Fig. 7C, left), they were efficiently and significantly suppressed by pre-treatment with Plant PeptoQ (Fig. 7C, right). For the *OsOPR7* overexpressor, the pattern was not that straightforward. In the absence of the Plant PeptoQ, the ground level (which was similar to that in the wild type), was sustained at moderate salt stress, and even reduced at stringent salt stress (Fig. 7C, left). Upon pre-treatment with the Plant PeptoQ, the superoxide levels decreased further, but only under salt stress. There was no effect in the absence of salt (Fig. 7C, right). Thus, while *OsOPR7* overexpression and Plant PeptoQ interacted additively under salt stress, the Plant PeptoQ did not modulate superoxide levels, if salt was absent.

When we measured the activities of superoxide dismutase, we found for the wild type, the decrease of activity under salt stress turned into an increase after pretreatment with Plant PeptoQ (Fig. 7D, right). The same held true for the *OsOPR7* overexpressor. However, the enzyme activities were equal to those seen for the wild type, although in the absence of the Plant PeptoQ, the SOD activities under salt stress remained high, while those of the wild type dropped (Fig. 7D, left). In the absence of salt stress, the enzymatic activities were more or less the same, independent of genotype, and independent of Plant PeptoQ treatment. Thus, the pattern of SOD activity is more or less a mirror image of the pattern for superoxide levels. Again, the interaction of the *OsOPR7* overxpression and Plant PeptoQ are not behaving additively. On the other hand, we investigated the activities of catalase, we found that it gets increased under salt stress irrespective of salt concentration in the absence of Plant PeptoQ as compared to the negative control, more or less in the same manner both in the WT and the *OsOPR7* overexpressor cell lines (**Suppl. Fig. S5A**). In the presence of Plant PeptoQ pretreatment, almost the same result was observed like the case in the absence of Plant PeptoQ. However, here, there is a significant difference between the WT and the *OsOPR7* overexpressor in the absence of salt stress where the CAT activities increased in the *OsOPR7* overexpressor unlike the case in the WT cell line (**Suppl. Fig. S5B**).

Likewise, we measured the levels of the precursor OPDA, JA, and the final product JA-Ile in Plant PeptoQ pretreated *OsOPR7* overexpressor and WT BY-2 cells after 1 and 3 h of salt stress. The Plant PeptoQ increased the resting levels of OPDA in the WT (for comparison, we added the values without the Plant PeptoQ in grey symbols in Fig. 8A**,** **B**). This difference ceased progressively under salt stress. Thus, Plant PeptoQ acted in the same way as did overexpression of *OsOPR7* (Fig. 8A**,** **B**). The combination of both factors did not add up, however. Upon Plant PeptoQ treatment, the resting levels of OPDA were significantly, by almost 50 %, lower in the *OsOPR7* overexpressor as compared to the WT (although they increased transiently under salt stress at 1 h but dropped back to the level of the WT at 3 h). This means that the effects of Plant PeptoQ and of *OsOPR7* overexpression neutralised each other. The level of JA-Ile in the wild type remained persistently at around 6 pmol g^{-1} fresh weight after addition of the Plant PeptoQ, independently of salt stress and time point (Fig. 8C**,** **D**). The ratio of JA-Ile over OPDA under salt stress was significantly lower in the WT when the Plant PeptoQ was present (Fig. 8E**,** **F**). The same holds true for the *OsOPR7* overexpressor, albeit to a lesser extent. This contrasts with the situation without Plant

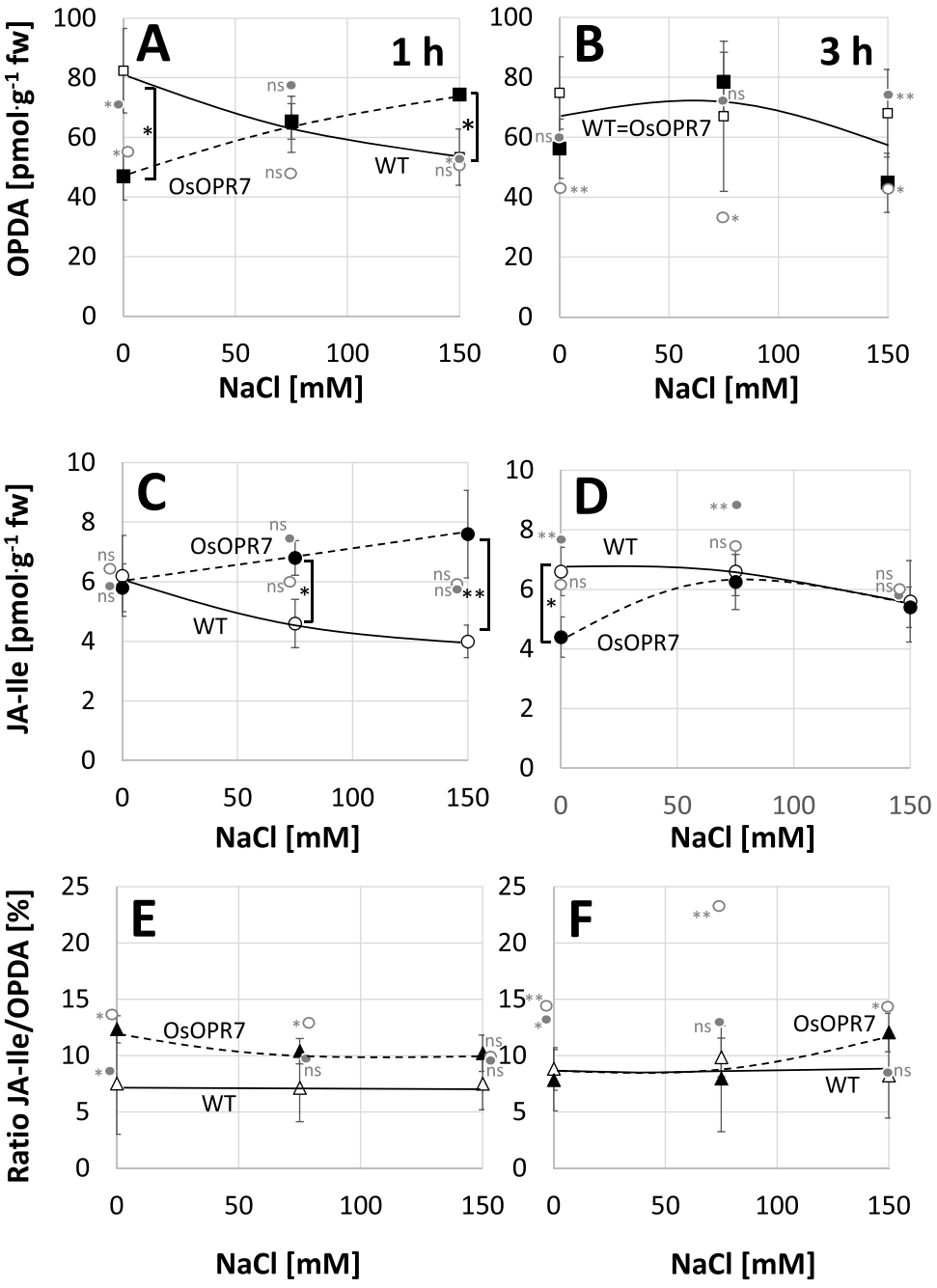

Fig. 8. Effect of salt stress on 12-oxo-phytodienoic acid (12-OPDA) and Jasmonic acid-isoleucine (JA-Ile) level as well as JA-Ile/OPDA (%) upon pretreatment with Plant PeptoQ. **A, B** The level of 12-OPDA in WT (grey curve) and *OsOPR7* overexpressor (broken curve) BY-2 cells. **C, D** The level of JA-Ile in WT (grey curve) and *OsOPR7* overexpressor (broken curve) BY-2 cells. **E, F** JA-Ile/OPDA (%) in WT (grey curve) and *OsOPR7* overexpressor (broken curve) BY-2 cells. Data represent mean values and standard errors of three independent experimental series. ** indicate differences significant at $P \leq 0.01$, * at $P \leq 0.01$ based on a Student's *t*-test.

PeptoQ, where the ratio of JA-Ile over OPDA turned out to be half as low in the *OsOPR7* overexpressor under salt stress (Fig. 6C). Again, the combination of Plant PeptoQ and *OsOPR7* overexpression did not add up, but more or less quelled each other.

Thus, both with respect to *SOD* transcript levels, superoxide dismutase activity, superoxide steady-state levels, and jasmonate levels, overexpression of *OsOPR7* and addition of Plant PeptoQ did not act additively, although they act at different subcellular locations.

3. Discussion

In the current work, we have addressed the role of ODPA reductase (OPR), the first peroxisomal enzyme in the jasmonate biosynthesis pathway, for the cellular response to salt stress. Our experimental model were tobacco BY-2 cells, overexpressing a GFP-fusion of *OPR7* from rice. We confirmed that the fusion protein correctly targets peroxisomes and steady-state levels for the respective transcript were by three orders of magnitude higher than the endogenous *OPR*. We found that this overexpression leads to a more robust oxidative balance, evident from a higher activity of superoxide dismutase (SOD), lower levels of superoxide and lipid peroxidation damage, along with a conspicuous and specific upregulation of mitochondrial SOD transcripts. Unexpectedly, the steady-state levels of OPDA were not decreased but increased and remained so under salt stress. We had seen a similar mitigation of salt stress upon treatment with the anti-oxidative, mitochondria-localised, cell-penetrating peptoid, Plant PeptoQ [36]. We tested, therefore, the combined effect of Plant PeptoQ and ectopic OsOPR7. Since they are targeting different organelles, their effect should be additive. However, this was not, what we observe. With respect to their effect on *NAC*, a factor involved in retrograde signalling from mitochondria to the nucleus, both factors appeared to act inversely. In the following, we will first discuss the role of OPDA and JA-Ile for salt adaptation, give an

explanation, why overexpression of *OPR7* leads to elevated (and not to lower) levels of OPDA, and develop a model how peroxisomes and mitochondria interact functionally to maintain oxidative homeostasis under salt stress. This model leads to implications that are testable by cell biological approaches.

3.1. Is OPR7 a switch between life and death?

In response to salt stress, cells can initiate adaptation, for instance, by activating the vacuolar sodium channel NHX1, sequestering sodium ions into the vacuole, such that ionic stress in the cytoplasm dissipates and turgescence persists. Alternatively, the challenged cell can initiate cell death, which is lethal for the individual cell, but sometimes beneficial for the plant as an entity. Older tissues can, thus, accumulate the salt and undergo abscission, such that the meristems remain vital, allowing regeneration of new organs once the stress period is over [15]. It seems that the choice between these two cellular strategies depends on the jasmonate pathway (reviewed in [6]). Using rice mutants with a loss of function in allene oxide cyclase (AOC), we could show in previous work [7] that a strong accumulation of OPDA (occurring in wild type rice in response to salt stress) correlates with necrosis. Mutants with a loss of function of AOC that are not able to synthetise OPDA can circumvent cell death and instead activate different events of cellular adaptation.

Does this mean that OPDA is a signal initiating cell death? If so, OPR7 would play the role of a cellular switch between life and death. A more efficient conversion of OPDA by the overexpressed *OPR7* should then improve cellular survival under salt stress. This is exactly what we observe when we analyse proliferation (Fig. 2), cell expansion (Fig. 3A), mortality (Fig. 3B), oxidative damage (Fig. 4A**, B**), or redox homeostasis (Fig. 4C**, D**). However, we do not see the expected decrease of OPDA steady-state levels, but we rather see an increase (Fig. 6A). We also do not see a significant increase of JA-Ile (Fig. 6B), as it should result from a more efficient partitioning of OPDA towards the peroxisomal conversion into JA. This outcome is surprising, given the fact that the GFP fusion of OsOPR7 localises to peroxisomes, as it should (Fig. 1), and that the steady-state transcript levels are more than 2000-fold higher than the endogenous *NtOPR* transcripts (Fig. 5C, **Suppl. Fig. S4F**).

While we will discuss the potential reasons for this paradox outcome in the following section of the discussion, we can state here already that obviously the notion that OPDA acts as a "death signal" cannot be true. Is it then the absence of JA-Ile in the *aoc* loss-of-function rice mutants that ensured their survival [7]? This would not hold for the current case, because JA-Ile levels do not differ significantly between the *OsOPR7* overexpressor and the wild type (Fig. 6B). Further evidence against the notion that JA-Ile *per se* acts as a "death signal" comes from a comparative study conducted in two grapevine cell lines differing with respect to salt tolerance, show that a rapid, but transient accumulation of JA-Ile correlates with efficient adaptation to salt stress [41]. Thus, it is not the mere presence or absence of OPDA, nor of JA-Ile as such that decide about the cellular response. Instead, the cell makes use of more complex inputs, such as temporal patterns or ratios between signals. We propose, therefore, a jasmonate signature model to explain the cellular decision of cellular adaptation versus necrosis.

To address a jasmonate signature hypothesis experimentally, is not trivial, but it is possible. To test the idea that a rapid, but transient activation of jasmonate signalling acts as signature for adaptation, we had engineered transgenic rice lines, where a salt-responsive promoter drove expression *OsJAZ8*, the jasmonate response regulator that is most responsive to salt stress in rice [42]. Under salt stress, jasmonate signalling would first ensue, but then remain transient, because the synthesis of the OsJAZ8 protein would rapidly quell the progression of JA signalling. In a variant of this approach, a dominant-negative version of *OsJAZ8* was engineered that, due to a lacking ZIM domain, would not undergo proteolysis. In fact, these transgenic lines exhibited a higher tolerance to salt stress, which was even higher in the lines expressing the dominant-negative version of *OsJAZ8*.

In case of tobacco cells, the steady-state levels of JA-Ile are much smaller (only around 15 %) of those for OPDA, meaning that only a fraction of OPDA is processed in the peroxisome (Fig. 6C). This ratio increases under salt stress in the wild type, but remains low in the *OPR7* overexpressor. Thus, OPDA might not be just a precursor for JA-Ile, but act as signal of its own virtue [13]. The decision between cellular adaptation and necrosis would then depend on the *balance* between JA-Ile triggered gene expression and OPDA-triggered responses.

Can we come up with a mechanistic model supporting such an OPDA-JA balance model? Yes, we can, because the role of JA for salt adaptation has two faces:

The current working model for the signalling role of OPDA ascribes a key role to the plastid localised receptor cyclophilin 20−3 (CYP20−3), which, upon binding of its ligand, OPDA, will recruit serine acetyltransferase (SAT) for cysteine synthesis [14]. SAT is a limiting factor for the activation of the cysteine synthase complex (CSC) and, thus, regulates sulfur assimilation [43,44]. As a result, binding of OPDA to CYP20−3 leads to increased production of cysteine through increased SAT activity [45]. The accumulating cysteine will convert to glutathione, modulating the redox potential in the plastid, which activates retrograde signalling culminating in the synthesis of TGA transcription factors, inducing OPDA-responsive genes, such as glutathione-S-transferases with a glutathione-peroxidase activity that act as ROS scavengers [14,46]. Thus, OPDA allows retrograde signalling from the plastid to the nucleus and the activation of adaptive gene expression to re-establish redox homeostasis in the plastid. In other words: OPDA, which is synthetised as result of lipid peroxidation (as it typically occurs under stress), is not only a precursor of jasmonates, but can act as damage signal by its own virtue. In line with implications from this hypothesis, increased OPDA levels in variegated leaves correlated with reduced ROS levels, at simultaneous accumulation of glutathione levels and induction of specific GSTs [46].

The final product of jasmonate synthesis, JA-Ile, deploys an independent chain of events leading to salt adaptation. A rapid, but transient pulse of JA-Ile signalling, activates abscisic-dependent responses such as the accumulation of compatible osmolytes (such as betaine or proline), but also protective proteins (such as dehydrins or late embryogenesis abundant proteins) that chaperone proteins and membranes from illegitimate aggregations (for review see [6]). However, a chronically elevated jasmonate level can result in cell death through uncoupling redox homeostasis in mitochondria as shown for roots [47], but also for leaves [48,49]. Peroxidase-like GSTs can mitigate this effect [50]. Upon overexpression, a GST with peroxidase activity improved the performance under oxidative stress [51]. The reduced glutathione forming the substrate of this reaction can enter the mitochondria through a still unknown transporter [29]. A straightforward hypothesis would be that JA impairs SOD activity in the mitochondria. OPDA-triggered signalling culminating in accumulation of GSTs with peroxidase activity would counteract this negative impact of JA-Ile accumulation.

Therefore, efficient adaptation to salt stress requires a defined balanced between OPDA and JA-Ile signalling. This leads to the next question. Overexpression of *OPR* should *reduce* the steady state levels of OPDA and, thus, the mitigation of the negative impact of JA-Ile signalling on mitochondrial redox homeostasis should become weaker, which should lead to reduced salinity tolerance. However, we observe an improved salinity tolerance, and our observations are in line with previous studies, where overexpression of wheat *OPR* in wheat itself or in Arabidopsis as heterologous system leads to higher salt tolerance [21].

The jasmonate pathway is generally activated in response to abiotic stress (reviewed in [12]) This does not necessarily come with an increase in the steady-state levels of JA. While JA was thought in the past to be the active hormone, it is meanwhile clear that it is only a precursor for the active hormone, the conjugate JA-Ile [8]. However, JA can also be methylated to generate the volatile MeJA, which acts as systemic stress signal and is, in the target tissue, metabolised into JA and JA-Ile again. Thus, the steady state level of JA depends on the conversion from OPDA

(input), the conjugation to JA-Ile (active signal) and methylation to MeJA (volatile systemic signal). In fact, we only were able to detect JA-Ile, along with the precursor OPDA, indicating that the conjugation occurs at a fast rate. It is not unusual that JA-Ile accumulates without a corresponding increase of JA, since this was already observed earlier in suspension cells from the grapevine *V. riparia* in response to salt stress [6].

3.2. How can overexpression of OPR7 lead to accumulation of OPDA?

The phenomenon that overexpression of *OPR* improves salt tolerance ([21]; the current study) would be easy to understand, if OPDA were a death signal. It becomes surprising, when OPDA triggers anti-oxidative mitigation [14]. However, our study revealed a second surprise: in contrast to the expectation, the overexpression of *OPR7* (by a factor of more than three orders of magnitude over the levels in the wild type) does not reduce the steady-state levels of OPDA, but rather leads to an increase. Is it possible to come up with an explanation for this apparently paradox result?

It is, if one considers that fact that OPDA needs to translocate from the plastid, the site of its synthesis, into the peroxisome, the site of its processing and the location of OPR7. The export from the plastid depends on the transporter JASSY [52], while the ATP-binding cassette transporter COMATOSE is responsible for the import into the peroxisome [53]. Since OPR7 enters the peroxisomal matrix by virtue of its peroxisomal import motif, its overexpression should recruit large parts of the transport machinery, such as docking proteins or components of the transport pore. This might interfere with the proper localisation of transporters (such as COMATOSE) in the peroxisomal membrane. That both systems interact is supported by findings that overexpression of proteins required for the targeting of peroxisomal membrane proteins, such as Pex3p, results in complete import failure of matrix proteins [54]. Thus, overexpression of *OsOPR7* might phenocopy a comatose loss-of-function mutant. Such mutants show significantly increased OPDA levels [53]. The limited import of substrate to the peroxisome would then override the effect of the elevated levels of OPR7 due to sequestering the substrate in a different compartment (the plastid).

There is an alternative explanation, though, coming from the discovery that OPRs fulfill a moonlighting function in redox homeostasis, by reducing mono-dehydro ascorbate to ascorbate [55]. This function would compete with the canonic role of OPRs as ODPA reductases. As a result, the conversion of OPDA would be impaired, while the regeneration of ascorbate would mitigate the oxidative stress in response to sodium. Thus, the increase of OPDA would be a by-product of an improved ascorbate cycle. A testable implication of this hypothesis would be elevated ascorbate levels under salt stress in the *OPR7* overexpressor cell line.

3.3. There is signaling from mitochondria to the peroxisomes

Plant PeptoQ can phenocopy *OsOPR7* overexpression with respect to its effect on mortality, superoxide steady-state levels, mitochondrial *MnSOD* transcripts, and hormone levels. This is surprising, since OsOPR7 acts on the level of plastid-peroxisomal interaction, while Plant PeptoQ localises to the mitochondria. If these effects were independent, an additive interaction should result. This is clearly not the case. Thus, there must be a functional interaction between the two organelles with respect to salt-induced oxidative stress. Such an interaction would be consistent with the literature record. Peroxisomes, chloroplasts, and mitochondria have membranous extensions called peroxules, stromules and matrixules respectively [56]. Peroxules form in response to oxidative stress [27] and link with other organelles that have close physical and metabolic ties, such as chloroplasts, mitochondria, endoplasmic reticulum, and oil bodies [27,28,57,58]. In photosynthetic tissue, a close association of chloroplasts, mitochondria and peroxisomes is characteristic for photorespiration [59]. Components of peroxisomal fission, such as FIS1, are also involved in mitochondrial division [60]. The components of the mitochondrial Krebs cycle and those of the oil-degrading glyoxysome cycle overlap, and both cycles join through transported metabolites such as citrate, succinate, or acetyl-carnitine [61]. In particular, peroxisomes can sense oxidative imbalance in other organelles. They respond by translocating to the perturbed site and detoxify excessive reactive oxygen species (for a review see [62]). As result of this interaction, the mitochondrial oxidative imbalance in consequence of salt stress dissipates. Whether Plant PeptoQ dissipates excessive ROS in the mitochondria or whether overexpressed *OsOPR7* promotes the ability of the peroxisome to detoxify the ROS accepted from the challenged mitochondrion (for instance, through improved ascorbate regeneration [55]) is equivalent with respect to its physiological consequence. However, since the interaction between both organelles depends on the level of oxidative stress, both factors do not simply add up, but are interdependent.

We arrive at the following working model that allows to explain the data of the current study and to deduce crucial questions for future research: Sodium ions can pass freely through the outer mitochondrial membrane into the inner mitochondrial membrane, where they perturb the respiratory electron transport chain leading to the formation of superoxide ions (Fig. 9, ①), which are converted by the mitochondrial Mn-associated superoxide dismutase (SOD) into hydrogen peroxide by the activity of superoxide dismutase (Fig. 9, ②). Plant PeptoQ specifically accumulates in the mitochondria and can accept the excess electrons from superoxide, restoring redox homeostasis (Fig. 9, ③). In parallel, Plant PeptoQ can deploy retrograde signalling to the nucleus (Fig. 9, ④) culminating in the expression and mitochondrial import of SOD, which further helps to restore redox homeostasis under challenge of sodium [36]. Under oxidative stress, peroxisomes, rich in catalase (CAT), move into the proximity of the challenged mitochondrion and detoxify hydrogen peroxide into water (Fig. 9, ⑤). In parallel to the mitochondria, sodium ions can also enter the stroma of the plastids, leading to peroxidation of poly-unsaturated fatty acids (PUFA) by the lipoxygenase (LOX), and, thus, deploying the jasmonate biosynthesis pathway leading to the accumulation of OPDA (Fig. 9, ⑥). Similarly to mitochondria, plastids and peroxisomes approach each other (possibly under the formation of stromules and/or peroxules), such that OPDA can reach the peroxisomal matrix through membrane channels, such as COMATOSE1. Here it is further converted by OPDA-Reductase and the subsequent enzymes into jasmonic acid (Fig. 9, ⑦), which leaves the peroxisome again and eventually yields bioactive JA-Ile. The same enzyme has a second function in regenerating ascorbate for scavenging of hydrogen peroxide and thus directly contributes to redox homeostasis. The recruitment of the peroxisomal localisation machinery for the excess of OPR7 might also impair the proper localisation of the OPDA import components such as COMATOSE1 (⑧).

This model has implications that explain several non-intuitive aspects of our results. For instance, the improved salt tolerance of the *OPR7* overexpressor is explained by the improved ascorbate recycling, which allows to detoxify reactive oxygen species from the mitochondria more efficiently. The recruitment of OPR7 for this function would also explain, why OPDA is not reduced under these circumstances. The non-additive interaction between Plant PeptoQ and *OPR7* overexpression would result from the fact that both factors mitigate salt-induced reactive oxygen species. Although this happens at two different sites (Plant PeptoQ: mitochondria; OPR7: peroxisome), they are functionally linked, because the detoxification of hydrogen peroxide, generated in the mitochondria, occurs in the peroxisome.

3.4. Outlook

Our current work indicates that redox homeostasis under salt stress depends on dynamic interactions between different organelles. These interactions might not only be of functional quality (such as the retrograde signalling from mitochondria to the nucleus, or the detoxification

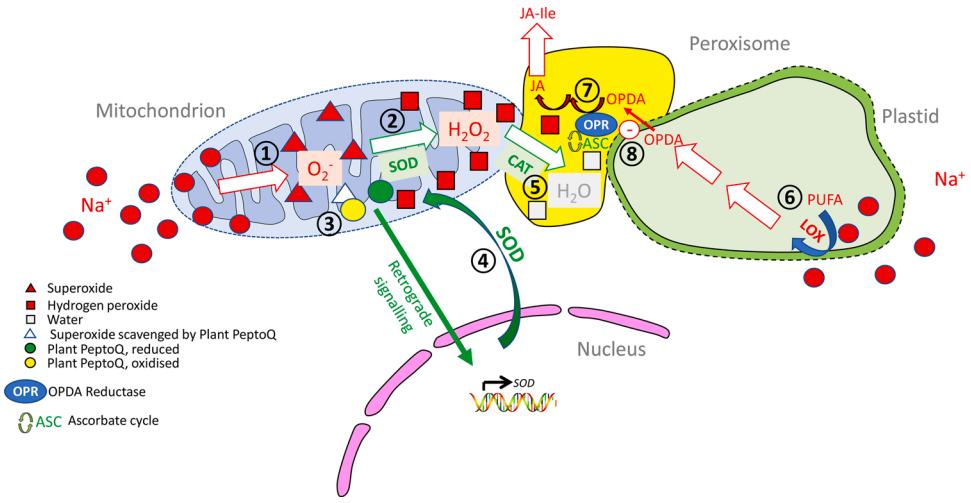

Fig. 9. Working model on the mode of action of Plant PeptoQ and OsOPR7, and the interaction among mitochondrion, peroxisomes and plastid. ① Sodium ions enter into the mitochondrial inner membrane, perturb the electron transport chain (ETC) and lead to the formation of superoxide ions. ② The generated superoxide ions are converted into hydrogen peroxide by the action of superoxide dismutase. ③ Furthermore, the superoxide ions are scavenged by Plant PeptoQ. ④ In parallel, Plant PeptoQ deploys retrograde signalling to the nucleus. ⑤ In the peroxisome, catalase (CAT) detoxifies hydrogen peroxide into water. ⑥ Sodium ions enter into the stroma of the plastids, cause the peroxidation of poly-unsaturated fatty acids (PUFA) by the lipoxygenase (LOX), and, thus, deploying the jasmonate biosynthesis pathway leading to the accumulation of OPDA. ⑦ The OPDA which is imported from plastids into peroxisome is converted into jasmonic acid by OPDA-Reductase and other subsequent enzymes where it leaves the peroxisome and eventually yields bioactive JA-Ile. ⑧ The recruitment of the peroxisomal localisation machinery for the excess of OPR7 might also impair the proper localisation of the OPDA import components such as COMATOSE1.

of hydrogen peroxide originating from the mitochondria by peroxisomes), but of topological nature. This would imply that the occurrence of organellar protrusions, such as stromules, might be a manifestation of stress compensation. How these protrusions form, is far from understood, but due to the close interaction of mitochondria with the actin cytoskeleton, an impact of contractile forces can be conceived. In ongoing experiments, we are currently testing this possibility. In these experiments, we use a fluorescent plastid marker and can observe, how salt stress is inducing stromules [for review see [63]), long protrusions of the plastids that get into touch with mitochondria and peroxisomes.

4. Materials and methods

4.1. Cell lines and cell cultivation

Discussed in [36]. For subcultivation, we added 1.5 mL of stationary cells as inoculum into 30 mL of fresh medium in a 100-mL Erlenmeyer flask. In case of the *OsOPR7*-GFP overexpressor, cells proliferated in the presence of hygromycin (60 mg L^{-1}). As a backup, we kept stock BY-2 calli on medium solidified with agar [0.8 % (w/v)] and subcultured them monthly.

4.2. Generating the OsOPR7 overexpression line

To get a stable overexpression line of *OsOPR7*-GFP in tobacco BY-2, we first isolated total RNA from coleoptiles of *Oryza sativa* ssp. Japonica cv. Dongjin with the innuPREP Plant RNA kit (Analytik Jena, Jena, Germany). After reverse transcription with the M-MuLV cDNA Synthesis Kit (New England Biolabs) according to the instructions of the manufacturer, the full-length coding sequence of *OsORP7* (accession number: LOC4345762) was amplified from the cDNA template by PCR using the oligonucleotide primers: attB1-OPR7 (forward primer): 5′-ACACCATATGGATCGGCCGCCGCCGGATCA-3′ and attB2-OPR7 (reverse primer): 5′-GTGTAAGCTTCATCCGCGACTTAGGCTGTCCGA -3′ with initial denaturation at 94 °C for 30 s, followed by 32 cycles of denaturation at 94 °C for 10 s, annealing at 71 °C for 20 s, and elongation at 72 °C for 45 s, terminated by a final elongation step at 72 °C for 2 min. Then, the PCR amplicon was integrated into the entry plasmid pENTR (Invitrogen), which after verification of the sequence, was then cloned into the binary GATEWAY vector pH7WGF2. This vector allows for C-terminal fusion of the green fluorescent protein, driven by the constitutive CaMV 35S promoter, and followed by hygromycin resistance. After verification of the sequence, the vector was then ready for stable transformation into tobacco BY-2 cell (*Nicotiana tabacum* L. cv Bright Yellow 2) using an Agrobacterium-mediated protocol [64]. The non-transformed tobacco BY-2 cell was referred to as WT BY-2. In some experiments, the peroxisomal marker *PTS1*-mCherry [37], a kind gift by Prof. Dr. Jaideep Mathur (Guelph University, Canada) was transformed into the *OsOPR7*-GFP overexpressor lines, using the same protocol, but without selection.

4.3. Determination of cell density

OsOPR7 overexpressor and non-transformed BY-2 cells were treated with 0, 75, or 150 mM NaCl during sub-cultivation, respectively. Discussed in [36].

4.4. Cell length and width measurement

OsOPR7 overexpressor and WT BY-2 cells were treated with 0, 75, or 150 mM NaCl, respectively, to measure cell length and cell width of the respective cells. Discussed in [36]. Cell width and length of the long cell axis were measured using the AxioVision software Rel. 4.8 (Zeiss) from composite images of the entire field using the MosaiX routine. Discussed in [36].

4.5. Determination of viability

To determine cell viability, 0.5 mL aliquots of cells treated with 0, 75, or 150 mM NaCl for both, WT and *OsOPR7* overexpressor cells were collected at 24, 48, 72, and 96 h after sub-cultivation. Discussed in [36].

4.6. Determination of lipid peroxidation

The product of lipid peroxidation, malonedialdehyde (MDA), was measured as indicator for oxidative burst using a reaction between MDA and 2-thiobarbituric acid (TBA) according to [65] with minor modifications as follows: *OsOPR7* overexpressor and WT BY-2 cells were treated at day 4 after sub-cultivation with 0, 75, or 150 mM NaCl, respectively, and samples were collected at 1 and 4 h by removing the medium using a vacuum pump to get about 100 mg of cells that were transferred to 2-ml reaction tubes and frozen in liquid nitrogen and kept

frozen till analysis. The exact fresh weight was determined prior to freezing by comparing the filled tube with an empty reaction tube. Discussed in [36].

4.7. Measurement of Superoxide, hydrogen peroxide, and activities of antioxidant enzymes

Discussed in [36].

4.8. Measurement of cellular Na^+ and K^+ content

Transgenic *OsOPR7* overexpressor and WT BY-2 cells were treated with 0, 75, or 150 mM NaCl, respectively, at day 4 after sub-cultivation and incubated on a shaker at 150 rpm. Discussed in [36]. The dried cell material was mixed in digestion tubes (Gerhardt, UK) with 5 mL of concentrated nitric acid (HNO_3) and then incubated for 24 h at room temperature incubation, whereby the samples were vortexed after 6 h and then, a second time, at the end of the 24-h interval. After incubation, samples were boiled in a water bath at 105 °C for 2 h, and after cooling, filled up to 10 mL with distilled water and mixed again by a vortex. Eventually, Na^+ and K^+ content was determined by flame atomic absorption spectrometry (AAnalyst200, Perkin Elmer) in an air-acetylene flame against blank samples, where 5 mL concentrated nitric acid had been added into an empty digestion vessel and processed in the same way as above to correct the measurements. Three independent biological replicates, each in technical triplicates were used to calculate cation concentration with reference to the dry weights.

4.9. Endogenous levels of OPDA, JA, and JA-Ile

Endogenous levels of OPDA, JA and JA-Ile were measured based on ultraperformance liquid chromatography–tandem mass spectrometry (UPLC-MS/MS) using [$^2H_5$] OPDA, [$^2H_6$] JA and [$^2H_2$] JA-Ile as standards according to [66].

4.10. RNA extraction and quantitative real-time PCR

Total RNA was isolated from WT and *OsOPR7* overexpressor BY-2 cells, treated with either 0, 75, or 150 mM NaCl, respectively. Discussed in [36].

Author contributions

K.G.A. designed the research, carried out all the experiments (except those conducted by R.E, E.E. and B.H.), prepared figures and wrote the manuscript. R.E. conducted SOD and CAT activity and *MnSOD* gene expression assays. E.E. performed cations level analysis. B.H. determined plant hormone levels. Q.L., S.P., S.A., R.D. and M.R. provided technical assistance to K.G.A. I.B. designed the Plant PeptoQ. S.W.M., I. W., S.B. and U.S. synthesized and characterized the Plant PeptoQ. P.N. conceived original concepts, drew Fig. 9, supervised and complemented the writing. K.G.A. agreed to act as the responsible author for contact and communication. All authors reviewed the manuscript and approved the final version before submission.

Funding

This work was supported by funding to KGA, RD and PN by the German-Egyptian Research Fund (GERF - 01DH14013), and the German Research Council (SFB1190) to IB. The work was further supported by the German research Foundation DFG by the RTG 2039 Molecular architecture for fluorescent cell imaging (IW, SWM, US, SB) and the Helmholtz Program Biointerface in Technology and Medicine.

Data availability

All data generated and analysed in the current study are available from the corresponding author on reasonable request.

Declaration of Competing Interest

The authors report no declarations of interest.

Acknowledgements

This work was supported by funds from the German-Egyptian Research Fund to KGA, RD and PN, and from the German Research Council for IB. We thank Hagen Stellmach (IPB Halle) for technical assistance in determination of jasmonates. Moreover, we thank Prof. Dr. Jaideep Mathur (Guelph University, Canada) for his kind donation of the peroxisomal marker *PTS1*-mCherry.

Appendix A. Supplementary data

Supplementary material related to this article can be found, in the online version, at doi:https://doi.org/10.1016/j.plantsci.2021.111156.

References

[1] J.T. Flowers, Improving crop salt tolerance, J. Exp. Bot. 55 (396) (2004) 307–319.
[2] R. Munns, M. Tester, Mechanisms of salinity tolerance, Annu. Rev. Plant Biol. 59 (2008) 651–681.
[3] J.-K. Zhu, Plant salt tolerance, Trends Plant Sci. 6 (2) (2001) 66–71.
[4] U. Deinlein, A.B. Stephan, T. Horie, W. Luo, G. Xu, J.I. Schroeder, Plant salt-tolerance mechanisms, Trends Plant Sci. 19 (6) (2014) 371–379.
[5] D. Golldack, C. Li, H. Mohan, N. Probst, Tolerance to drought and salt stress in plants: unraveling the signaling networks, Front. Plant Sci. 5 (151) (2014) 1–10.
[6] A. Ismail, S. Takeda, P. Nick, Life and death under salt stress: same players, different timing? J. Exp. Bot. 65 (12) (2014) 2963–2979.
[7] M. Hazman, B. Hause, E. Eiche, P. Nick, M. Riemann, Increased tolerance to salt stress in OPDA-deficient rice ALLENE OXIDE CYCLASE mutants is linked to an increased ROS-scavenging activity, J. Exp. Bot. 66 (11) (2015) 3339–3352.
[8] C. Wasternack, S. Song, Jasmonates: biosynthesis, metabolism, and signaling by proteins activating and repressing transcription, J. Exp. Bot. 68 (6) (2017) 1303–1321.
[9] B. Vanholme, W. Grunewald, A. Bateman, T. Kohchi, G. Gheysen, The tify family previously known as ZIM, Trends Plant Sci. 12 (6) (2007) 239–244.
[10] A. Chini, S. Fonseca, G. Fernandez, B. Adie, J.M. Chico, O. Lorenzo, G. Garcia-Casado, I. Lopez-Vidriero, F.M. Lozano, M.R. Ponce, J.L. Micol, R. Solano, The JAZ family of repressors is the missing link in jasmonate signaling, Nature 448 (2007) 666–671.
[11] A. Wager, J. Browse, Social network: JAZ protein interactions expand our knowledge of jasmonate signaling, Front. Plant Sci. 3 (41) (2012) 1–11.
[12] M. Riemann, R. Dhakarey, M. Hazman, B. Miro, A. Kohli, P. Nick, Exploring jasmonates in the hormonal network of drought and salinity responses, Front. Plant Sci. 6 (1077) (2015) 1–16.
[13] N. Taki, Y. Sasaki-Sekimoto, T. Obayashi, A. Kikuta, K. Kobayashi, T. Ainai, K. Yagi, N. Sakurai, H. Suzuki, T. Masuda, K.I. Takamiya, D. Shibata, Y. Kobayashi, H. Ohta, 12-Oxo-phytodienoic acid triggers expression of a distinct set of genes and plays a role in wound-induced gene expression in Arabidopsis, Plant Physiol. 139 (2005) 1268–1283.
[14] S.W. Park, W. Li, A. Viehhauser, B. He, S. Kim, A.K. Nilsson, M.X. Andersson, J. D. Kittle, M.M.R. Ambavaram, S. Luan, A.R. Esker, D. Tholl, D. Cimini, M. Ellerström, G. Coaker, T.K. Mitchell, A. Pereira, K.J. Dietz, C.B. Lawrence, Cyclophilin 20-3 relays a 12-oxo-phytodienoic acid signal during stress responsive regulation of cellular redox homeostasis, PNAS 110 (23) (2013) 9559–9564.
[15] J.-Y. Li, A.-L. Jiang, W. Zhang, Salt stress-induced programmed cell death in rice root tip cells, J. Integr. Plant Biol. 49 (4) (2007) 481–486.
[16] F. Schaller, E.W. Weiler, Molecular cloning and characterization of 12-Oxophytodienoate reductase, an enzyme of the octadecanoid signaling pathway from Arabidopsis thaliana, J. Biol. Chem. 272 (44) (1997) 28066–28072.
[17] F. Schaller, P. Hennig, E.W. Weiler, 12-Oxophytodienoate-10,11-Reductase: Occurrence of two isoenzymes of different specificity against stereoisomers of 12-Oxophytodienoic acid, Plant Physiol. 118 (1998) 1345–1351.
[18] F. Schaller, C. Biesgen, C. Müssig, T. Altmann, E.W. Weiler, 12-Oxophytodienoate reductase 3 (OPR3) is the isoenzyme involved in jasmonate biosynthesis, Planta 210 (2000) 979–984.
[19] J. Strassner, A. Fürholz, P. Macheroux, N. Amrhein, A. Schaller, A homolog of old yellow enzyme in tomato, J. Biol. Chem. 274 (49) (1999) 35067–35073.
[20] T. Tani, H. Sobajima, K. Okada, T. Chujo, S.I. Arimura, N. Tsutsumi, M. Nishimura, H. Seto, H. Nojiri, H. Yamane, IdentiWcation of the OsOPR7 gene encoding 12-

oxophytodienoate reductase involved in the biosynthesis of jasmonic acid in rice, Planta 227 (2008) 517–526.
[21] W. Dong, M. Wang, F. Xu, T. Quan, K. Peng, L. Xiao, G. Xia, Wheat oxophytodienoate reductase gene TaOPR1 confers salinity tolerance via enhancement of abscisic acid signaling and reactive oxygen species scavenging, Plant Physiol. 161 (2013) 1217–1228.
[22] N. Shai, M. Schuldiner, E. Zalckvar, No peroxisome is an island — peroxisome contact sites, Biochim. Biophys. Acta 1863 (2016) 1061–1069.
[23] N. Kaur, S. Reumann, H.J. Jianping, Peroxisome biogenesis and function, Am. Soc. Plant Biol. (2009) 1–41.
[24] R.J.A. Wanders, H.R. Waterham, S. Ferdinandusse, Metabolic interplay between peroxisomes and other subcellular organelles including mitochondria and the endoplasmic reticulum, Front. Cell Dev. Biol. 3 (83) (2016) 1–15.
[25] K. Oikawa, M. Hayashi, Y. Hayashi, M. Nishimura, Re-evaluation of physical interaction between plant peroxisomes and other organelles using live-cell imaging techniques, J. Integr. Plant Biol. 61 (7) (2019) 836–852.
[26] T. Su, W. Li, P. Wang, C. Ma, Dynamics of peroxisome homeostasis and its role in stress response and signaling in plants, Front. Plant Sci. 10 (705) (2019) 1–14.
[27] A.M. Sinclair, C.P. Trobacher, N. Mathur, J.S. Greenwood, J. Mathur, Peroxule extension over ER-defined paths constitutes a rapid subcellular response to hydroxyl stress, Plant J. 59 (2009) 231–242.
[28] E.-A. Jaipargas, N. Mathur, F.B. Daher, G.O. Wasteneys, J. Mathur, High light intensity leads to increased peroxule-mitochondria interactions in plants, Front. Cell Dev. Biol. 4 (6) (2016) 1–11.
[29] G. Noctor, C.H. Foyer, Intracellular redox compartmentation and ROS-related communication in regulation and signaling, Plant Physiol. 171 (2016) 1581–1592.
[30] R. Pan, J. Liu, S. Wang, J. Hu, Peroxisomes: versatile organelles with diverse roles in plants, New Phytol. 225 (2019) 1410–1427.
[31] L. Shumbe, A. Chevalier, B. Legeret, L. Taconnat, F. Monnet, M. Havaux, Singlet oxygen-induced cell death in Arabidopsis under high-light stress is controlled by OXI1 Kinase, Plant Physiol. 170 (2016) 1757–1771.
[32] S. Ng, I. De Clercq, O. Van Aken, S.R. Law, A. Ivanova, P. Willems, E. Giraud, F. Van Breusegem, J. Whelan, Anterograde and retrograde regulation of nuclear genes encoding mitochondrial proteins during growth, development, and stress, Mol. Plant 7 (2014) 1075–1093.
[33] N.E. Blanco, M. Guinea-Diaz, J. Whelan, A. Strand, Interaction between plastid and mitochondrial retrograde signaling pathways during changes to plastid redox status, Philos. Trans. Biol. Sci. 369 (2014) 1–8.
[34] K. Bobik, T.M. Burch-Smith, Chloroplast signaling within, between and beyond cells, Front. Plant Sci. 6 (781) (2015) 1–26.
[35] K.G. Asfaw, Q. Liu, J. Maisch, S.W. Münch, I. Wehl, S. Bräse, I. Bogeski, U. Schepers, P. Nick, A peptoid delivers CoQ-derivative to plant Mitochondria via endocytosis, Sci. Rep. 9 (2019) 9839.
[36] K.G. Asfaw, Q. Liu, X. Xu, C. Manz, S. Purper, R. Eghbalian, S.W. Münch, I. Wehl, S. Bräse, E. Eiche, B. Hause, I. Bogeski, U. Schepers, M. Riemann, P. Nick, A mitochondria-targeted coenzyme Q peptoid induces superoxide dismutase and alleviates salinity stress in plant cells, Sci. Rep. 10 (2020) 11563.
[37] S.L.K. Ching, S.K. Gidda, A. Rochon, O.R. van Cauwenberghe, B.J. Shelp, R. T. Mullen, Glyoxylate reductase isoform 1 is localized in the cytosol and not peroxisomes in plant cells, J. Integr. Plant Biol. 54 (3) (2012) 152–168.
[38] H. Buschmann, P. Green, A. Sambade, J.H. Doonan, C.W. Lloyd, Cytoskeletal dynamics in interphase, mitosis and cytokinesis analysed through Agrobacterium-mediated transient transformation of tobacco BY-2 cells, New Phytol. 190 (2011) 258–267.
[39] E.P. Glenn, J.J. Brown, Salt tolerance and crop potential of halophytes, Crit. Rev. Plant Sci. 18 (2) (1999) 227–255.
[40] R.L. Heath, L. Packer, Photoperoxidation in isolated chloroplasts I.KInetics and stoichiometry of fatty acid peroxidation, Arch. Biochem. Biophys. 125 (1968) 189–198.
[41] A. Ismail, M. Seo, Y. Takebayashi, Y. Kamiya, E. Eiche, P. Nick, Salt adaptation requires efficient fine-tuning of jasmonate signaling, Protoplasma 251 (2012) 881–898.
[42] K.P. Peethambaran, R. Glenz, S. Höninger, S.M.S. Islam, S. Hummel, K. Harter, Ü. Kolukisaoglu, D. Meynard, E. Guiderdoni, P. Nick, M. Riemann, Salt-inducible expression of OsJAZ8 improves resilience against salt-stress, BMC Plant Biol. 18 (311) (2018) 1–15.
[43] J.R. Dominguez-Solis, Z. He, A. Lima, J. Ting, B.B. Buchanan, S. Luan, A cyclophilin links redox and light signals to cysteine biosynthesis and stress responses in chloroplasts, PNAS 105 (42) (2008) 16386–16391.
[44] H. Takahashi, S. Kopriva, M. Giordano, K. Saito, R. Hell, Sulfur assimilation in photosynthetic organisms: molecular functions and regulations of transporters and assimilatory enzymes, Annu. Rev. Plant Biol. 62 (2011) 157–184.
[45] A. Blaszczyk, R. Brodzik, A. Sirko, Increased resistance to oxidative stress in transgenic tobacco plants overexpressing bacterial serine acetyltransferase, Plant J. 20 (2) (1999) 237–243.
[46] Y.H. Sun, C.Y. Hung, J. Qiu, J. Chen, F.S. Kittur, C.E. Oldham, R.J. Henny, K. O. Burkey, L. Fan, J. Xie, Accumulation of high OPDA level correlates with reduced ROS and elevated GSH benefiting white cell survival in variegated leaves, Sci. Rep. 7 (2017) 44158.
[47] V.M. Loyola-Vargas, E. Ruíz-may, R.M. Galaz-Ávalos, C. De-la-Peña, The role of jasmonic acid in root mitochondria disruption, Plant Signal. Behav. 7 (6) (2012) 611–614.
[48] A.M.D.S. Soares, T.F. de Souza, T. Jacinto, O.L.T. Machado, Effect of methyl jasmonate on antioxidative enzyme activities and on the contents of ROS and H2O2 in Ricinus communis leaves, Braz. J. Plant Physiol. 22 (3) (2010) 151–158.
[49] L. Zhang, D. Xing, Methyl jasmonate induces production of reactive oxygen species and alterations in mitochondrial dynamics that precede photosynthetic dysfunction and subsequent cell death, Plant Cell Physiol. 49 (7) (2008) 1092–1111.
[50] D.B. Bartling, R. Radzio, U. Steiner, E.W. Weiler, A glutathione S-transferase with glutathione-peroxidase activity from Arabidopsis thaliana. Molecular cloning and functional characterization, Eur. J. Biochem. 216 (1993) 579–586.
[51] V.P. Roxas, R.K. Smith, E.R. Allen, R.D. Allen, Overexpression of glutathione S-transferase/glutathione peroxidase enhances the growth of transgenic tobacco seedlings during stress, Nat. Biotechnol. 15 (1997) 988–991.
[52] L. Guan, N. Denkert, A. Eisaa, M. Lehmann, I. Sjuts, A. Weiberg, J. Solla, M. Meinecke, S. Schwenkert, JASSY, a chloroplast outer membrane protein required for jasmonate biosynthesis, PNAS 116 (21) (2019) 10568–10575.
[53] F.L. Theodoulou, K. Job, S.P. Slocombe, S. Footitt, M. Holdsworth, A. Baker, T. R. Larson, I.A. Graham, Jasmonic acid levels are reduced in COMATOSE ATP-binding cassette transporter mutants. Implications for transport of jasmonate precursors into peroxisomes, Plant Physiol. 137 (2005) 835–840.
[54] R.J.S. Baerends, F.A. Salomons, K.N. Faber, J.A.K.W. Kiel, I.J. van de Klei, M. Veenhuis, Deviant Pex3p levels affect normal peroxisome formation in Hansenula polymorpha: high steady-state levels of the protein fully abolish Matrix Protein Import, Yeast 13 (15) (1997) 1437–1448.
[55] D. Maynard, V. Kumar, J. Sproß, K.-J. Dietz, 12-Oxophytodienoic acid reductase 3 (OPR3) functions as NADPH-dependent α,β-Ketoalkene reductase in detoxification and monodehydroascorbate reductase in redox homeostasis, Plant Cell Physiol. 61 (3) (2020) 584–595.
[56] I. Scott, I.A. Sparkes, D.C. Logan, The missing link: inter-organellar connections in mitochondria and peroxisomes? Trends Plant Sci. 12 (9) (2007) 380–381.
[57] N. Thazar-Poulot, M. Miquel, I. Fobis-Loisy, T. Gaude, Peroxisome extensions deliver the Arabidopsis SDP1 lipase to oil bodies, PNAS 112 (13) (2015) 4158–4163.
[58] H. Gao, J. Metz, N.A. Teanby, A.D. Ward, S.W. Botchway, B. Coles, M.R. Pollard, I. Sparkes, In vivo quantification of peroxisome tethering to chloroplasts in tobacco epidermal cells using optical tweezers, Plant Physiol. 170 (2016) 263–272.
[59] J. Hu, A. Baker, B. Bartel, N. Linka, R.T. Mullen, S. Reumann, B.K. Zolman, Plant peroxisomes: biogenesis and function, Plant Cell 24 (2012) 2279–2303.
[60] I. Scott, A.K. Tobin, D.C. Logan, BIGYIN, an orthologue of human and yeast FIS1 genes functions in the control of mitochondrial size and number in Arabidopsis thaliana, J. Exp. Bot. 57 (6) (2006) 1275–1280.
[61] M. Pyc, Y. Cai, M.S. Greer, O. Yurchenko, K.D. Chapman, J.M. Dyer, R.T. Mullen, Turning over a new leaf in lipid droplet biology, Trends Plant Sci. 22 (7) (2017) 596–609.
[62] M.L. Sandalio, M.C. Romero-Puertas, Peroxisomes sense and respond to environmental cues by regulating ROS and RNS signalling networks, Ann. Bot. 116 (2015) 475–485.
[63] M.H. Schattat, K.A. Barton, J. Mathur, The myth of interconnected plastids and related phenomena, Protoplasma 252 (2015) 359–371.
[64] J. Klotz, P. Nick, A novel actin–microtubule cross-linking kinesin, NtKCH, functions in cell expansion and division, New Phytol. 193 (2012) 576–589.
[65] F.D. Gaff, O. Okong'O-Ogola, The use of non-permeating pigments for testing the survival of cells, J. Exp. Bot. 22 (1971) 756–758.
[66] G.U. Balcke, V. Handrick, N. Bergau, M. Fichtner, A. Henning, H. Stellmach, A. Tissier, B. Hause, A. Frolov, An UPLC-MS/MS method for highly sensitive high-throughput analysis of phytohormones in plant tissues, Plant Methods 8 (47) (2012) 1–11.